

FACTORS FOR INTERACTIVE LIQUID PERCEPTION IN  
AUGMENTED REALITY ON MOBILE DEVICES

BRANDON FUNG

A THESIS SUBMITTED TO  
THE FACULTY OF GRADUATE STUDIES  
IN PARTIAL FULFILLMENT OF THE REQUIREMENTS  
FOR THE DEGREE OF  
MASTER OF APPLIED SCIENCE

GRADUATE PROGRAM IN ELECTRICAL ENGINEERING AND COMPUTER  
SCIENCE

YORK UNIVERSITY  
TORONTO, ONTARIO

JANUARY 2019

© Brandon Fung 2019

# ABSTRACT

Augmented reality (AR) is one of the hottest things with Apple and Google trying to capture people's interests and wonder. Given these new needs, there have not been much on what the best thing to do when creating these experiences. Thus in my work, I investigate the best way to bring believable virtual interactive liquids into the real world . Believability is what the user would feel is a more representative of a liquid in real life even when the liquid is virtual. Therefore, I examine three factors for virtual liquids, namely the dynamics and texturing of the liquid and the real world lighting. This works finds that motion models are the most important factor for humans to believe that the virtual fluid in AR is a liquid regardless of angles. This allow developers to focus on the motion models rather than any other factors when creating new experiences in AR.

# Acknowledgments

I would like to thank my family for their support and Mark Rosewater for being the head Designer at Wizards of the Coast for Magic: the Gathering. Also reddit user /u/AutumnStudios.

# Contents

|   |            |
|---|------------|
| <b>ABSTRACT</b>   | <b>ii</b>  |
| <b>Acknowledgments</b>                                      | <b>iii</b> |
| <b>1 Introduction</b>                                       | <b>1</b>   |
| 1.1 Motivations . . . . .                                   | 4          |
| 1.2 Overview . . . . .                                      | 4          |
| <b>2 Factors influencing realistic AR fluid simulations</b> | <b>6</b>   |
| 2.1 Lighting . . . . .                                      | 6          |
| 2.2 Textures . . . . .                                      | 10         |
| 2.3 Dynamics . . . . .                                      | 12         |
| <b>3 Liquid Dynamic Models</b>                              | <b>16</b>  |
| 3.1 Wave Equation . . . . .                                 | 17         |
| 3.2 Wave Particle . . . . .                                 | 19         |
| 3.2.1 Formulation . . . . .                                 | 20         |
| 3.3 iWave . . . . .   | 26         |
| 3.3.1 Wave Equation Convolution . . . . .                   | 26         |
| 3.3.2 Wave Implementation . . . . .                         | 31         |
| <b>4 Experiments and Results</b>                            | <b>34</b>  |
| 4.1 Hypotheses . . . . .                                    | 34         |
| 4.2 Methods . . . . .                                       | 35         |

|          |                                     |           |
|----------|-------------------------------------|-----------|
| 4.3      | Experimental Design . . . . .       | 40        |
| 4.3.1    | Environment and Procedure . . . . . | 41        |
| 4.3.2    | Questions . . . . .                 | 43        |
| 4.4      | Data Analysis . . . . .             | 45        |
| 4.4.1    | Data . . . . .                      | 45        |
| 4.4.2    | Analysis . . . . .                  | 50        |
| 4.4.3    | Discussion . . . . .                | 58        |
| <b>5</b> | <b>Conclusion</b>                   | <b>61</b> |
| 5.1      | Future Work . . . . .               | 61        |
| 5.2      | Concluding Remarks . . . . .        | 64        |
|          | <b>References</b>                   | <b>65</b> |

# List of Tables

|     |  |    |
|-----|--|----|
| 4.1 | Notation . . . . .   | 45 |
| 4.2 | Pairs for experiment questions one through three . . . . . | 50 |
| 4.3 | Pairs for experiment Question 4 . . . . .                  | 50 |
| 4.4 | Model coefficients . . . . .                               | 52 |
| 4.5 | Wilcoxon Dynamic Comparison of mean . . . . .              | 55 |
| 4.6 | Wilcoxon Texture Comparison of mean . . . . .              | 56 |
| 4.7 | Wilcoxon Lighting Comparison of mean . . . . .             | 58 |
| 4.8 | Wilcoxon question four results . . . . .                   | 58 |

# List of Figures

|      |  |    |
|------|--|----|
| 3.1  | Wave equation graphs . . . . .                             | 19 |
| 3.2  | Diagram of wave particle changing the surface . . . . .    | 20 |
| 3.3  | Single particle render . . . . .                           | 22 |
| 3.4  | Multiple particle render . . . . .                         | 22 |
| 3.5  | Curve wavefront diagram . . . . .                          | 23 |
| 3.6  | Subdivision and no subdivision comparison . . . . .        | 24 |
| 3.7  | How to subdivide diagram . . . . .                         | 25 |
| 3.8  | Lattice quantization diagram . . . . .                     | 31 |
| 4.1  | User view of experiment . . . . .                          | 36 |
| 4.2  | Development demo image . . . . .                           | 37 |
| 4.3  | Image targets for Vuforia . . . . .                        | 38 |
| 4.4  | Picture of hardware . . . . .                              | 39 |
| 4.5  | iWave Stimuli . . . . .                                    | 40 |
| 4.6  | Wave Particle Stimuli . . . . .                            | 41 |
| 4.7  | View on one side of experiment . . . . .                   | 42 |
| 4.8  | Image of how the experiment was done by the user . . . . . | 45 |
| 4.9  | Experiment flow chart diagram . . . . .                    | 46 |
| 4.10 | Question 1 response histogram . . . . .                    | 47 |
| 4.11 | Question 2 response histogram . . . . .                    | 48 |
| 4.12 | Question 3 response histogram . . . . .                    | 48 |
| 4.13 | Question 4 response histogram . . . . .                    | 49 |

# Chapter 1

## Introduction

In today's technologically shifting landscape, new technologies are constantly springing up and are allowing never before seen interactions to exist. One area of technology that is booming in recent years is virtual reality which is enabled by new economical head mounted displays. Similarly, augmented reality (AR) experiences, especially involving mobile devices such as the iPhone's AR kit (Apple, 2018) and Androids ARCore (Google, 2018a), have been garnering commercial and research interest as of late. The public are also becoming accustomed to using their mobile devices as head mounted displays (HMD) through add-ons. These economical devices such as the Google cardboard (Google, 2018b) and Samsung's viewer (Samsung, 2018) enable virtual reality experiences to a wider audience. New innovations and public acceptance leads to more demand for augmented reality experiences through the HMD, but currently there is a lack of perceptual studies using these technologies.

With current AR technologies, the user can see the real world with virtual objects placed in their environment. Users can interact with them just as if they were

present in the real life environment while not physically there. Notable examples of such experiences are the Hololens AR headset developed by Microsoft (Kress & Cummings, 2017) and the Magic Leap HMD (Magic Leap, 2018). These new promising technologies are exciting but to create a convincing AR experience requires diverse understandings. These include technological limitations and how AR can result in a perceptual difference between virtual objects and reality.

One difference between AR experiences, compared to things like movie animations, is the need for real-time computations. This need for real-time computations was illustrated by Debevec (Debevec, 1998) in which lighting was considered for augmented reality. He pointed out that if the environment suddenly changes, like turning off the lights, the appearance of the virtual object must also account for this change and adjust itself to compensate . This highlights another issue in which the interactions in AR must conform with causal expectations assumed in the real world environment. If the virtual object remains lit in a dark room, then one would see that the object does not conform with the illumination in the room which has an affect on believability as shown by (Kan, Dunser, Billinghurst, Schonauer, & Kaufmann, 2014).

As more applications get made, it seems natural that some of these applications would include liquid interaction. Creating such experiences with liquids in classical graphics would typically involve modeling the liquids through a fluid simulation as detailed in (Bridson, 2015). Simulating liquids comes with its own limitations as this thesis will discuss. This is especially true when one starts to interact with a fluid, for example pouring liquid in a pool of liquid or having objects impact a body of liquid. To have convincing liquid simulations would require a lot of computing power due to

the non-rigid motion liquids exhibit. Thus to do AR on a mobile device through a HMD, I have identified a few constraints that should be considered when constructing the liquid-object interactions.

- **Computing the dynamics in real time:**

In games, most interactions are in real time, namely when the user interacts with objects in the scene. Since the study takes place in an AR environment, similar techniques are used since when the user interacts with the virtual objects, for a fluid experience, it must be in real time. This poses the constraint that one cannot use pre-computed animations for the liquid-object interaction.

- **Interaction with real environment:**

In AR, the key constraint is to populate real world environments with virtual objects. To do so, one needs to determine both what is to be rendered and what information from the real environment is required to render the object. This leads to a constraint in which the object must be perceived to be actually in the room and not an artifact from the viewing device.

- **Hardware Constraints:**

Since my augmented reality environment is going to be experienced through a mobile device, I must carefully consider the resources that the simulations consume. This is especially an issue because the mobile phone is mounted on the face. Hence, I want to ensure that phone does not overheat which could cause discomfort to the user. Thus, when making the simulations, I should strive to have efficient algorithms and/or methods to put operations on the

GPU when necessary to limit potential risks.

## 1.1 Motivations

With these constraints, I want to determine which factors of a liquid-interaction simulation have the largest effect in the perception of liquids in an AR environment. Answering this question could help evaluate design decisions when creating similar interactions for AR applications. Such human factors data informs the application developer about what portion of the interaction to focus attention and resources on.

The three factors of the liquid-interaction I explore are (1) the dynamics of liquid-interaction, (2) the skinning or texturing of the liquid and (3) the environmental lighting of the liquid interacting with the lighting of the virtual object. It should be noted that the both lighting and texturing are not computationally intensive for the phone and the most computationally intensive portion is the dynamic simulation. To study liquid interaction, I will be studying how the liquid interacts with a virtual object.

## 1.2 Overview

Chapter 2, reviews the literature that has studied the factors we are exploring: lighting, texturing and dynamics. In chapter 3, I will discuss in detail the physical models that were used in the experiments, going over derivations as well as explaining how they were implemented. Chapter 4 gives the hypothesis of our experiments and outlines the experiment that was conducted as well as the analysis of the data taken.

In the final section, I will discuss future directions of research and identify some experimental limitations that could be addressed in the future.

# Chapter 2

## Factors influencing realistic AR fluid simulations

### 2.1 Lighting

In this section I will review previous studies that investigate how lighting of scenes affects different perception of believability of virtual objects in augmented reality. As well as how lighting is perceived in liquid scenes in a computer graphics environment.

In augmented reality environments, the environment lighting is not generated on the computer so the renderer does not have knowledge of how the lighting in the scene could change. This is a problem because in an extreme case, if a virtual object is lit in a dark room, it could greatly reduce believability that the object is indeed in the room. There have been systems developed to account for this issue such as the work of (Debevec, 1998), but an open question that remains is how much of our perceptual system are affected by these discrepancies. In the example posed, it is quite obvious

that there is an issue, but what if the differences were more subtle between the virtual lighting and environmental lighting. Could using better algorithms mask any ambiguities produced by these subtle differences? Several researchers have answered these questions in conventional graphics.

Kan et al (Kan et al., 2014) addressed the question of the role of algorithms on masking ambiguities between environmental and virtual lighting by comparing the perceptual difference between global illumination and direct illumination in an AR environment. The definition of direct illumination is when the object is only illuminated from the light source. The definition of global illumination is illumination that also considers reflections of light from other objects as well as the light source. To study the impact of these algorithms, an experiment comparing real objects with their virtual object counterparts was conducted. The virtual objects were lit using global or direct illumination in the virtual environment. The user compared two objects, one real and one virtual and choose which one was the real object. The users then answered questions about what they just saw. The authors formulated several hypotheses. They hypothesized that global illumination would deceive more people than direct illumination. Their hypothesis was supported by their data, which meant that having an accurate illumination model, in this case a global one, had a positive effect on perception in rendering virtual objects in AR.

Hattenberger, Fairchild, Johnson, and Salvaggio (2009) asked the same question but also developed a psychophysical model to determine how different illumination algorithms would be perceived in an AR scene. This allows for comparing different algorithms to predict which render appears to be more realistic. To build this model,

the authors had participants compare a real scene with an augmented scene. This was done by building a scene where a virtual cow was inserted into real environment rendered with various illumination algorithms. Since they required a real scene, they also constructed a physical cow and took a picture of the scene with the cow inserted physically instead of virtually. The authors described and investigated a range of lighting techniques that were used such as direct illumination techniques (e.g. direct illumination and whitted shading) to global illumination techniques (e.g. irradiance caching and photon mapping). Each of these techniques are used to approximate the bidirectional reflectance distribution function (Nicodemus, 1965) which renders the light in a virtual scene. For their experiment, participants were given a reference photo, the real scene, and two images that had the virtual cow inserted rendered with two different lighting algorithms. For those images, the participants were asked which of the two rendered images looked most like the reference. The authors found that global illumination methods that account for indirect illumination were preferred over direct methods. Since global illumination models real world lighting more closely than direct lighting, this result implies the closer to the real life lighting we get in a virtual model, the more the object appears realistic.

Knecht, Dünser, Traxler, Wimmer, and Grasset (2011) asked the question, what part of illumination can be removed by investigating the influence of shadows in AR on perceived depth and layout. This differs from (Kan et al., 2014) since it had the user do a physical task rather than a comparison task. Virtual cubes were generated randomly and the user had to estimate their apparent distance using the separation of their fingers as a metric. They found that the illumination methods had no effect on the users' judgments of the distances. If different lighting conditions did not have

an effect in a similar augmented reality setup to ours, then it is possible that this may also hold for liquid simulations.

These papers suggest that illumination fidelity has an influence on how people view the virtual objects. I wish to see if these patterns extend to the perception of believability on liquid interactions. Note that the work above only discussed solid objects without deforming surfaces. In the work below I discuss how lighting of water has an affect on perceiving liquids. This is of interest because it can provide insight on the differences between a dynamic liquid simulation in AR and static objects in AR as discussed above.

Bojrab, Abdul-Massih, and Benes (2013) focused their investigations on the caustics of water which is how light is reflected and refracted when hitting a body of transparent water. They explored the perceptual impact of situations where an illumination component was missing or replaced. Calculating illumination is typically an expensive task. Thus, if one can replace or substitute a component of the lighting rendering pipeline with a cheaper substitute with little perceivable visual degradation, then the results would have the same visual effect at a lower computational cost. To find out which component can be removed or replaced, the authors proposed seven components in scene of lighting materials to be studied. These include material specific like colour or transparencies and lighting specific properties like shadows. The material properties were varied by setting it to be transparent, a grey color, a blue color and transparent with refraction of light. The lighting properties varied by including hard and soft shadows of the water, caustics, and specular reflection. Four animated scenes were used in the evaluation. Each animation had a different property

altered or removed. Each scene with all the alterations were shown to the participant along with a control which had all properties included in the rendering process. The user then sorted the images in order of quality. What the authors found was that for all scenes, there was no statistically significant difference between animations with no shadow rendering and the control which implies that when rendering water, shadows do not have to be considered. They claim this could have a 20% speed up in rendering time for water based scenes.

These studies provide a baseline of what has been done on virtual environments on screen as well as augmented environments on computer monitor screens. While previous work suggests that when dealing with AR illumination of virtual objects, it is crucial for believability to use global illumination (Kan et al., 2014; Hattenberger et al., 2009), shadows do not play a huge role in physical tasks as well as in rendering water for computer graphics (Bojrab et al., 2013; Knecht et al., 2011). However, most of this work on illumination was conducted on stationary objects. Even when there was movement involved or perceived movement, one portion of lighting, shadows, did not have an effect on people's perception or performance. This leads to the question of whether these results can be replicated or apply in our setup namely a liquid interaction in augmented reality.

## **2.2 Textures**

Another property of virtual objects that could affect perception is the material or texture/skinning of the virtual object. There has not been a lot of augmented reality

experiments concerning this virtual property however this property has been studied in computer graphics. (Fleming, Wiebel, & Gegenfurtner, 2013) and (van Assen & Fleming, 2016) have asked: is our bias to attribute physical properties of objects based on their visual properties affect our expectation or understanding of other perceived physical properties of those virtual objects? I am interested in this question because we wish to see if texturing has an effect on perceiving motion and if it affects perceived perception of realism for virtual objects. By studying rigid interactions, we can see if those ideas also are transferred to non-rigid interactions.

For solid objects with textures modelled on real life objects like wood or rocks, the work of Fleming et al (Fleming et al., 2013) asked how do the visible material qualities of a solid object affect how people perceive its inherent physical properties. One example of this bias is how humans might see a ruffled object and perceive that object as being soft. To answer this question, showed users images from various real world materials such as wood or plastics and the participants would evaluate the objects properties based on what they saw. The properties the authors used were five visual properties of the object, namely glossiness, transparency, colorfulness, prettiness, and naturalness as well as four more physical properties like roughness, hardness, coldness and fragility. Overall the authors found users made consistent judgments of physical qualities based on only their visual material qualities. The authors concluded that there is a "strong coupling between visual prediction of material qualities and human understanding of the materials".

van Assen et al (van Assen & Fleming, 2016) extended this earlier experiment (Fleming et al., 2013), by studying a physical property of liquids, in their case was

viscosity, to see if optical properties such as texture, color, and glossiness had an effect on how people perceive the viscosity of liquids. More specifically, they wanted to see if the visual properties of the virtual fluid would have an affect on how people rate a liquid's viscosity, a physical property. To do this, the authors had a rating and a matching task when participants were shown a liquid with some viscosity and some set of optical properties. The participants had to adjust the viscosity of another liquid with different optical properties so they would match. To ensure that users were not simply matching the movement of the liquid, the two animations were shown at different points in time of the animation, thus ensuring that only the perception of viscosity was present. What the authors found was that users were able to match viscosities regardless of the visual appearance. The results imply that surface properties have no effect when perceiving different liquids with different viscosities.

Given most of these works uses standard workstations common in computer graphics, it is hard to conclude if different texturing, such as plain textures or pool/dirty water texture, would have an effect in augmented reality. Since computing power on a mobile phone is limited it would be of interest to determine if the findings for pure computer graphics also hold in AR environments. Thus, I predict that having texture would have an affect on believability as it will be outlined later in the hypotheses section.

## **2.3 Dynamics**

The most important aspects of a liquid simulator is how a liquid is physically simulated. Ideally, high fidelity models such as smooth particle hydrodynamics (SPH)

(Gingold & Monaghan, 1977) or fluid implicit particle (FLIP) (Brackbill, Kothe, & Ruppel, 1988) would be the best but at the cost of high computation times. These models are commonly used in computer graphics where SPH also is referred to as a particle method or Lagrangian method such as (Yuksel, 2010). These methods are described as representing the liquid as a collection of particles and moving each particle through the Navier-Stokes equation. The alternative would be a Eulerian method, such as (Tessendorf, 2004) in which you still move a liquid however this movement is parametrized on a grid. That is to say, all the information used to move the liquid is stored in the grid points and thus simulated by moving the grid points (Bridson, 2015).

The work presented below compares various liquid simulators with different computational costs. Some simulators are low in cost as explored in (Bates, Battaglia, Yildirim, & Tenenbaum, 2015) while (Um, Hu, & Thuerey, 2017) explored more state of the art models. The work presented below gives a brief introduction to what has already been done as well as how authors in the graphics community evaluate algorithm performance based on human responses.

The work of Um et al, (Um et al., 2017) asked how the differences between different simulated liquid dynamic models are perceived by humans, namely, how visually accurate are some models compared to others. The authors constructed the following framework to answer aspects of the question. A participant viewed two scenes undergoing some dynamics and picked whichever one was the closest representation of real dynamics. Some of the comparisons had a reference video of the motion that the animations were based on and some did not. The authors also had a transparent and

opaque condition for the liquid. For their simulation, they had two scenes differing in dynamics, one was the breaking dam setup, where a dam of water would have been removed in a tank and water would flow out, while the other one was a sloshing wave setup, a wave sloshing around a tank. The participants chose which scene they wanted to view. The authors constructed four experiments using this framework to compare the different dynamic models. Each experiment tackled a different set of conditions asking the general question of what were the differences between different the models. The questions of interest to us are the two experiments they did to find out which were the most visually accurate simulation. When asking which method produced the most visually accurate simulation, they showed that the SPH method was preferred. When asking which method produced the most visually accurate simulation under limited computing resources, Eulerian methods were preferred. This gives an idea of what methods to use under limited computing resources as well as a framework on how to construct the experiment.

An example of comparing physical simulation, solving equations based on physics, versus heuristic based simulation, using a pattern to simulate a liquids, is in the work of (Bates et al., 2015). The authors wanted to see whether an accurately simulated liquid was closer to human expectation than liquid movement based on following a heuristic or learned pattern. This was inspired by the Noisy Newton Hypothesis which hypothesizes that humans have an implicit knowledge of physics which allows them to know whether or not an interaction was modeled correctly through physics rather than heuristics. The authors extended the work on Newtonian physics (Smith, Battaglia, & Vul, 2013) to the topic of fluids to see if humans have the same mechanism for fluids as they seem to for rigid body physics. The authors completed their study with

the following experiment. They had a falling column of water which was modeled using SPH, a common fluid dynamical model, then used two models of propagation, a heuristic based model to dictate the movement of SPH particles and actually solving Navier Stokes equation which is normally done. What the authors found was that the participants expectations were correlated closer to the physically accurate simulation rather than the heuristic methods. Thus, it was perhaps quite difficult to fool human viewers with less accurate fluid simulations. It should be noted that all of these experiments were taken on a liquid crystal display which is stationary instead of having movement. Hence, our work extend this for different types of displays and environments.

Although my work does not use the exact methods that were studied in the earlier papers ,(Um et al., 2017; Bates et al., 2015), the previous work provides an experimental framework, i.e. comparison, to build upon. (Um et al., 2017) compared different fluid dynamical models with each other while (Bates et al., 2015) compared fluid dynamical models with simpler heuristic based models. These earlier results give the impression that true physical simulation is required and simplified models are not sufficient. We use wave equations approximations that are simpler than full dynamics models but higher fidelity than simpler heuristics for our comparisons. These techniques will be described in great detail in the next chapter.

# Chapter 3

## Liquid Dynamic Models

In my work, I am simulating a virtual liquid surface in augmented reality since when interacting with the fluid, only the surface is seen by the user. Therefore, simulating a virtual liquid boils down to simulating the wave equation (Yuksel, 2010; Canabal et al., 2016; Tessendorf, 2004). Ideally, the chosen method would be stable, not have aberrations, be fast enough for real time simulations, and work efficiently to avoid overworking the phone. The methods that are discussed in this thesis do not have all these desired qualities and therefore have pros and cons to their suitability. For instance, while the iWAVE by (Tessendorf, 2004) is smooth, has no noise or perturbations, it uses a lot of computing power, performing worse as time goes on. While the method of (Yuksel, 2010) is efficient and can run for a long period of time, the simulation has some noise, due to the nature of the implementation of the method.

In this section, I will review the calculation techniques that were used in my experiment which are detailed in (Yuksel, 2010; Tessendorf, 2004). I will start by giving a description of the types of dynamic models we are using, namely the wave

equation. Next, I will discuss the two methods used in greater detail including their implementation.

### 3.1 Wave Equation

Fluid dynamics have been studied in depth (Bridson, 2015; Gingold & Monaghan, 1977; Chentanez & Müller, 2010). Typically for high-fidelity liquid dynamics simulations, the authors model the dynamics through the Navier-Stokes equation (Fleming et al., 2013; Bates et al., 2015; Lee & O’Sullivan, 2007). Solving these equations requires the use of computers with a lot of processing power. Typically the approach to solving these equations can range from powerful graphics cards for very small simulations to rendering farms which are commonly used in movie production.

In our experiments, we are primarily interested in the object-liquid interaction. Ideally, to get the most exact solution, we would solve the 3-d Navier-Stokes equation. However, this is not computationally viable on a current mobile device in real time. Typically in object-liquid interaction, one would be concerned with visual changes to the liquid surfaces such as splashes, air bubbles and waves. There are also unobserved dynamics under the liquid such as vorticity in the lower layers of the liquid. Since we are primarily concerned with the interaction between the surface and objects, we can ignore non-visible features of the liquid simulation as well as splashes, and air bubbles since calculating these would require more computation. Thus instead of solving the Navier-Stokes equations along with other components that would be included in a dynamic liquid simulation, one would solve a problem that is related but much simpler computationally.

This study uses a simplification to the original problem of solving the Navier-Stokes equation by modelling the dynamics through the wave equation instead which is illustrated in equation 3.1. The wave equation has been studied extensively and is known to have a closed solution under some boundary conditions (Bridson, 2015). It should be noted, that since the wave equation is just the second derivative of time and space numerical solutions have been studied (Eriksson, Esterp, Hansbo, & Johnson, 1996). Due to waves dissipating in real life, it is necessary to add a dampening term thus we solve the wave equation with damping. This effect is illustrated in figure 3.1 in which over time, the waves would be smaller in amplitude.

$$\frac{\partial^2 h(x, y, t)}{\partial t^2} + \alpha \frac{\partial h(x, y, t)}{\partial t} = \nabla^2 h(x, y, t) \quad (3.1)$$

The wave equation (equation 3.1) includes a temporal derivative as well as spatial second derivatives for the oscillations which contributes to the oscillations of the wave equation along with a single spatial derivative multiplied by a dampening factor, advection, contributing to the dissipation of the wave. In equation 3.1, we have the term  $h$  as the height of the surface and  $\alpha$  as the damping factor, with  $x$  and  $y$  being the spatial position. In my study, I used two known ways of solving this problem based on the wave equation, the first method being wave particles by (Yuksel, 2010) and the second method iWave by (Tessendorf, 2008, 2004).

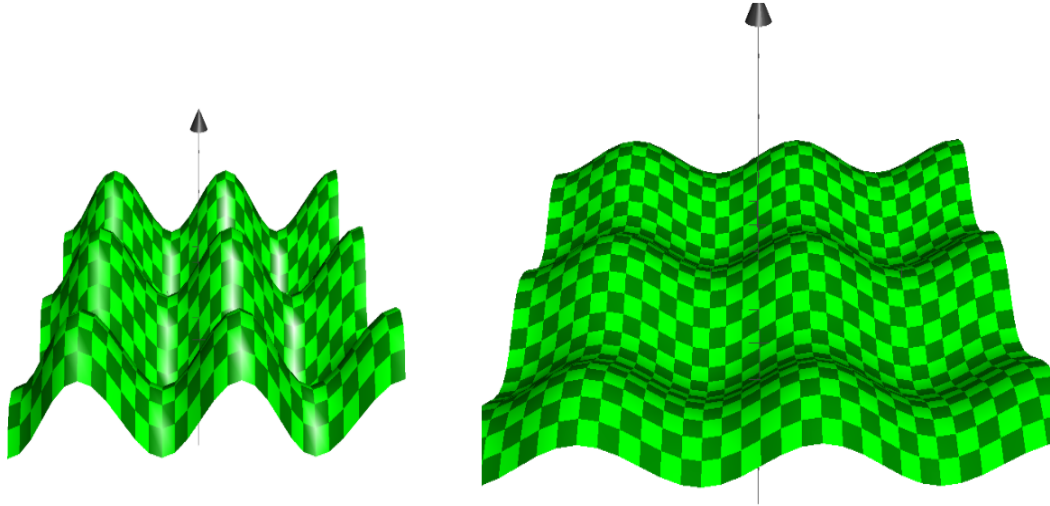


**Figure 3.1:** An example of a solution to equation 3.1, the wave equation, where the one on the left represents the wave at an initial fixed time,  $t_0$ , where the axes represent the spatial dimensions. At the beginning of the interaction (left) and after one time step with alpha being equal to one (right plot).

## 3.2 Wave Particle

In this section we will discuss the method of wave particles by (Yuksel, 2010). This method was motivated by proposing a real time water simulation that captures important visual components of a subset of water (Yuksel, 2010). This method allows for faster computation of a object-liquid interaction since one does not need to model the entire fluid body in order to accurately model an interaction. Using the wave particle method, one models the object-liquid interaction independent of any other information. This independence makes it easy to compute in parallel. In this section we will define the wave particle as well as discuss some implementation details.

### 3.2.1 Formulation

In the dissertation by (Yuksel, 2010), the goal was to determine the surface deviations that are caused by an object interaction. (Yuksel, 2010) proposed that just modelling the deviation on the liquid surface is sufficient. Each deviation on the liquid surface is modelled by a set of particles where each particle is assigned a deviation function dependant on the position on the liquid surface. Therefore, the whole dynamics of the system can be written as

$$Z(x, y, t) = z_0 + \eta_z(x, y, t) \quad (3.2)$$

$$\eta_z(x, y, t) = \sum_{i=1} D_i(x, y, t) \quad (3.3)$$

where  $Z$  is the height of the surface at a given point,  $(x, y)$  and time,  $t$ .  $\eta_z$  is the

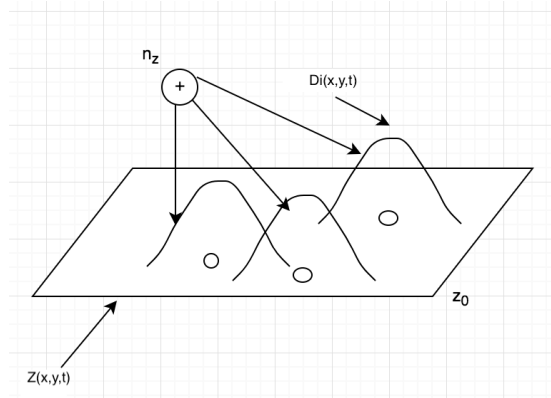


**Figure 3.2:** This shows the representation of the wave particle on a surface and how the equations 3.2 and 3.3 would deform the surface. It should be noted that  $\eta_z$  represents the summation of all the individual deformations

total deviation of the surface caused by all particles whereas  $D_i$  is the deviation of the surface at the same point and time for the  $i$ th particle. From this formulation,

(Yuksel, 2010) showed the solution is indeed a solution to the wave equation.

The dynamics of these particles are constrained on the surface and as noted in (Yuksel, 2010), where each particle represents a small surface deviation such that when summed can produce a wave effect. To do so, he models the deviation  $D$  from one particle as a clipped sinusoidal function for particle  $i$ , as shown in equation 3.4 and 3.5 and illustrated in figure 3.3.

$$W_i(u) = \frac{1}{2}(\cos\left(\frac{2\pi u}{\lambda_i}\right) + 1)\Pi\left(\frac{u}{\lambda_i}\right) \quad (3.4)$$

$$D_i(x, t) = a_i W_i(u) B_i(v) \quad (3.5)$$

Where  $\lambda_i$  is the desired wavelength of the wave, with  $u = \hat{u}_i(x(t) - x_i(t)) \hat{u}_i$  being the propagation direction, (i.e. the direction the particle is travelling) and  $v = \hat{u}_i^\perp(x(t) - x_i(t)) \hat{u}_i^\perp$  is the direction orthogonal to  $u$ ,  $x$  being the current position,  $x_i$  being the previous position and  $\Pi$  is a rectangle window function with lengths of  $u/\lambda_i$ . In this case,  $B_i(v)$  is a blending function used to ensure coherence between the addition of all the particles.

To create a 'wave' they used the fact that when summing together sinusoidal functions that differ by a translation in space, one could get an elongated sinusoidal function with a different amplitude. Thus, when multiple particles are near each other in a co-linear fashion, they would overlap and look like a wave front like in figure 3.4.

As one can see from figure 3.4, linear wavefronts are implemented in a line which is easier to implement, however in reality not all waves and dynamics can be modelled by linear wavefronts. Curved wavefronts are more common with the wave fronts either

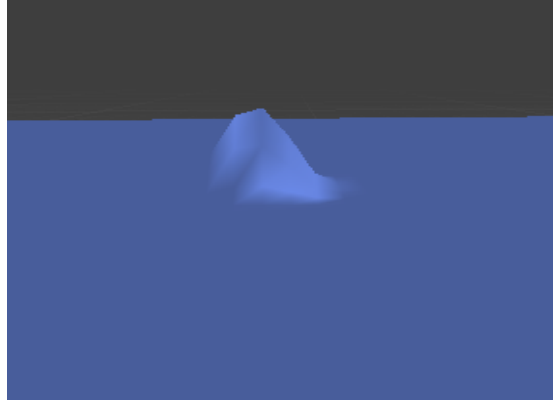


**Figure 3.3:** A render of how one particle would look in Unity rendered onto the surface described by equation 3

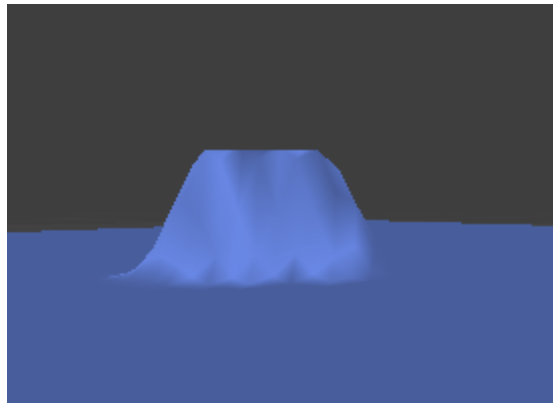


**Figure 3.4:** When multiple particles are beside each other, they superimpose in a co-linear fashion. In this case, there are three particles beside each other in a co-linear fashion deforming the surface to produce a wall that is curved near the edges.

expanding or contracting over time.

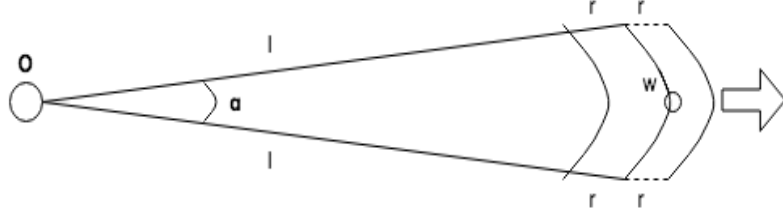


**Figure 3.5:** A figure adapted from (Yuksel, 2010) in which O is the origin of a particle such that the particle is a distance  $l$  away where the particle itself has a radius  $r$

Thus to create curved waves, the particles would be placed on the perimeter of a circle centered at a shared origin with some angular spacing, called the dispersion angle. From this we can derive a relationship between the angle of dispersion and the distance the particle has traveled from the origin as shown in equation 3.6 which follows figure 3.5, where  $\alpha$  is the dispersion angle,  $l$  is the distance from the particle to the origin and  $w$  is the arc length between two neighbouring particles. This is due to arc length calculation.

$$\frac{1}{l} = \frac{\alpha}{w} \quad (3.6)$$

From equation 3.7, one can find the exact position of each particle as long as it is active by the following equation where  $u$  is the propagation of a particle  $i$ .

$$(x_i, y_i) = O + lu \quad (3.7)$$

With the definition of the wave particle from origin, equation 3.7 and radial equation

3.6, one can rewrite equation 3.5 as

$$D_i(x, t) = \frac{a_i}{2} \left( \cos\left(\frac{\pi|x - x(t)|}{l_i}\right) + 1 \right) \Pi\left(\frac{|x - x_i(t)|}{l_i}\right) \quad (3.8)$$

with everything substituted in and where  $r_i$  is the wavelength of the sinusoidal in which is called the radius of the wave particle, and  $x$  is the location being estimated and  $x_i$  is the current position of propagating particle  $i$ .

With the radial formulation, an issue that occurs is that as time goes on, the particles become farther apart from each other and lose coherence. This issue is illustrated in figure 3.6 where on the right side the circular wave becomes a circle of peaks. One way to do this is after neighbouring particles are some distance apart, I would subdivide the particle into three new particles such that one previous wave particle would be equal to one old wave particle. This division is referred to as a **subdivision**.

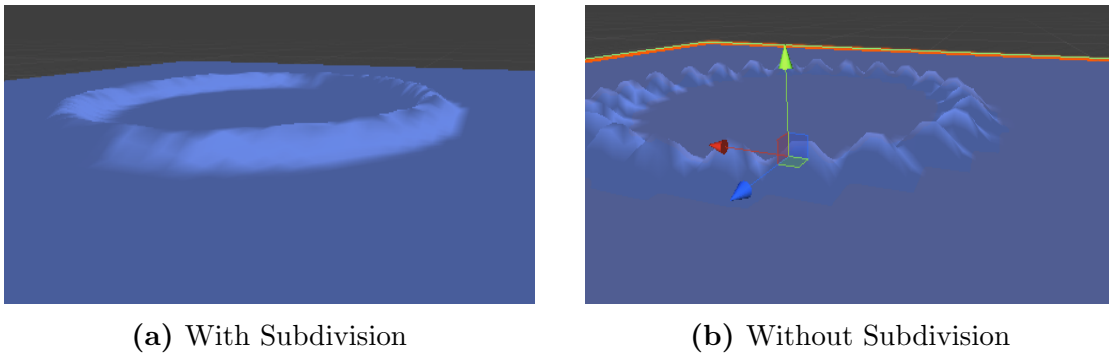


**Figure 3.6:** On the right, it is demonstrated how the particles will look without subdivision and on the left shows a smoother picture with the particles subdividing after some time.

To calculate when a subdivision should happen, as well as the position of the particle, consider the following. Suppose the particle,  $i$ , moves with velocity  $v$ . It can

be calculated where that particle would be after some time with equation 3.7. Then to ensure that we obtain figure 3.6a instead of 3.6b, when two adjacent particles,  $P_1$  and  $P_2$ , are a distance  $r$  apart such that two peaks could be seen, a third particle can be put in-between as shown in figure 3.7.

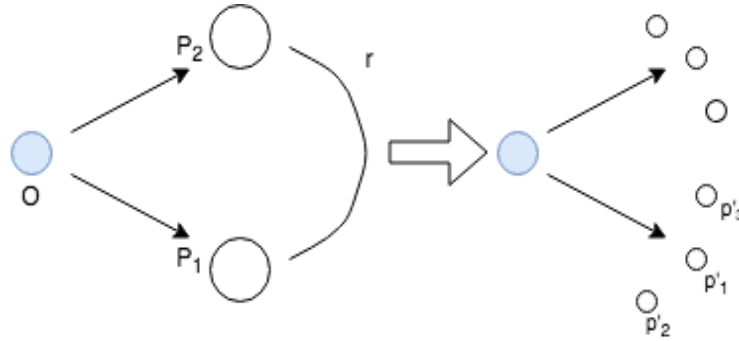


**Figure 3.7:** This diagram, adapted from (Yuksel, 2010) shows how the subdivision process is done starting from a Particle  $P_1$  with amplitude  $A$ , is subdivided into three particles with smaller amplitude where  $p'_1$  is in the same position with  $p'_2$  and  $p'_3$  beside it. As noted  $P_2$  is also subdivided with all new particles having the same origin,  $O$ , as well.

For implementation purposes, we insert two particles, one from each previous particle  $P_1$  and  $P_2$ . When a subdivision occurs, these new particles will have properties that are derived from their parent particle. The first is the amplitude  $a_i$  of each new particle,  $p_1, p_2$  and  $p_3$ , is one third the amplitude of the parent particle  $P_1$ . This is so there is amplitude coherence, i.e. the sum of the amplitudes for  $p_1, p_2$  and  $p_3$  would be the same as  $P_1$ . The second is due to having new particles, the dispersion angle for each new particle,  $p_1, p_2$  and  $p_3$ , would be changed to one third of the previous angle. The origin of each new particle would stay the same as the parent particle. This keeps each new particle independent from each another which makes it straight forward compute in parallel.

Subdivisions gives a dampening effect to the wave because amplitude is divided by three every subdivision. Therefore, if the amplitude of the resultant particle is so small such that the deviation for it is minimal, then the particle is removed. This typically occurs after a particle has undergone three subdivisions from when the whole interaction was first created. The particle is removed since the amplitude is very small.

Wave particles are created when an object interacts with the surface so for our experiments we have a simple implementation. We have a ball dropped on the surface making a circular wave. This causes a ring to be generated with the origin being the point of impact of the ball, thus providing a wave-like pattern as the interaction.

### **3.3 iWave**

iWave is a method provided by Tessendorf using kernel methods(Tessendorf, 2004; Canabal et al., 2016) i.e., using an effect function convolved with the surface for the effect. It should be noted that later authors built on the same idea of using kernel functions but used different kernel functions to produce different effects as described by (Canabal et al., 2016). In this section we will cover the main convolution operator that models portions of the wave equation and also parts of the implementation (Tessendorf, 2004, 2008; Nordeus, Erik, 2018).

#### **3.3.1 Wave Equation Convolution**

This method uses the wave equation to simulate the waves hence the equation

$$\frac{\partial^2 h(x, y, t)}{\partial t^2} + \alpha \frac{\partial h(x, y, t)}{\partial t} = -g \sqrt{\nabla^2 h(x, y, t)} \quad (3.9)$$

is used to simulate linear waves. This equation differs slightly from the classical wave equation with damping presented equation 3.1 due to the addition of a gravity term in the spatial derivative as well as the square root operation on the second spatial derivative, Laplacian. In this section we will provide the way the author discretized the spatial derivative using convolutions.

Consider a function  $f(x)$ , where  $f(x)$  is the height of the surface at some x-y position of the surface. Then consider the linear operation of taking the second derivative. From the theory of differential equations the linear transformation has the Fourier exponential functions for eigenfunctions and have corresponding eigenvalues being the value negative k squared as shown in equation 3.10.

$$\hat{e}_k(x) = \frac{1}{\sqrt{2\pi}} e^{ikx} \quad (3.10)$$

then the derivatives would be

$$\begin{aligned} \frac{d\hat{e}_k(x)}{dx} &= ik\hat{e}_k(x) \\ \frac{d^2\hat{e}_k(x)}{dx^2} &= -k^2\hat{e}_k(x) \\ \sqrt{\frac{d^2}{dx^2}}\hat{e}_k(x) &= |k|\hat{e}_k(x) \end{aligned} \quad (3.11)$$

By Fourier representation, any function  $f$  can be written as an integration as follows by  $k$  where it is integrated over the whole real line,  $\mathbb{R}$

$$f(x) = \int_{\mathbb{R}} \hat{e}_k(x) \hat{f}(x) dk \quad (3.12)$$

Then square root of the second derivative with respect to the position would be as follows from equation 3.11 and 3.12.

$$\sqrt{\frac{d^2}{dx^2}}\hat{f}(x) = \int_R |k|\hat{e}_k(x)\hat{f}(x)dk \quad (3.13)$$

When dealing with the position on a surface i.e., 2-dimensions instead of one, it is clear the the gradient operator extends naturally, with the only difference being that the eigenfunctions, equation 3.14, have a dot product of  $k$  and the two dimensional position of the function,  $\mathbf{x}$ , in the exponential term instead of regular multiplication you have in equation 3.10 which is only in one dimension. We also have something similar in 2-dimensions for the derivatives, equation 3.13, where the 2 dimensional version, equation 3.15 is the same as equation 3.13 except we have a new Fourier transformed function, and integrating over  $R^2$ .

$$\hat{e}_k(x) = \frac{1}{\sqrt{2\pi}}e^{ik \cdot x} \quad (3.14)$$

$$\sqrt{\frac{d^2}{dx^2} + \frac{d^2}{dz^2}}f(x) = \int_{R^2} |k|\hat{e}_k(x)\hat{\phi}(x)d^2k \quad (3.15)$$

When we consider the function  $f$  again in equation 3.15, then due to the properties of the Dirac delta (Mallat, 1999), one can rewrite it as an integral with a Dirac delta integrating of the the whole surface as shown in equation 16.

$$\int_{R^2} |k|\hat{e}_k(x)\hat{\phi}(x)d^2k = \int_R |k|\hat{e}_k(x)d^2k \int_{R^2} \hat{\phi}(q)\delta(k - q)d^2q \quad (3.16)$$

Since we have a delta function, then by orthogonality we can write it as an inner

product of the different arguments over another area.

$$\int_{R^2} \hat{\phi}(q) \delta(k - q) d^2q = \int_{R^2} \hat{\phi}(q) \int_{R^2} \hat{e}_k^*(y) \hat{e}_q(y) d^2y \quad (3.17)$$

By rearrangement of substituting 3.17 in 3.16

$$\int_{R^2} d^2y \int_{R^2} |k| \hat{e}_k^*(y) \hat{e}_q(x) d^2k \int_{R^2} \hat{\phi}(q) \hat{e}_q(y) d^2q \quad (3.18)$$

Since we have an inner product like structure with the Fourier basis functions, then we rename it as the kernel G dependent on the subtraction of x and y.

$$G(x - y) = \int_{R^2} |k| \hat{e}_k^*(y) \hat{e}_q(x) d^2k \quad (3.19)$$

Which would then lead to the equation being a convolution between a kernel G and the function  $\phi$

$$\int_{R^2} G(x - y) \hat{\phi}(y) d^2y \quad (3.20)$$

since

$$\int_{R^2} \hat{\phi}(q) \hat{e}_q(y) d^2q = \hat{\phi}(y) \quad (3.21)$$

For computational ease, the author adds a Gaussian term to the kernel, to smooth it out since the positions far away from the position x and y would have little effect on the end result, thus one can have a mathematical definition for not considering values outside of a range centered on (x,y).

$$G(x - y) = \int_{R^2} |k| \hat{e}_k^*(y) \hat{e}_q(x) e^{-|k|^2 \sigma^2} d^2k \quad (3.22)$$

Since we are working with circular waves, we can work with polar coordinates instead of Cartesian coordinates. Thus since equation 3.22 has been written as a convolution, consider what G looks like by taking y to be 0.

$$G(x) = \int_{R^2} |k| \hat{e}_q e^{-|k|^2 \sigma^2} d^2 k \quad (3.23)$$

Then one would use a change of variable from Cartesian to polar which would result in

$$G(x) = \int_0^\infty r e^{-r^2 \sigma^2} dr \int_0^{2\pi} r e^{ir|x|\cos(\theta)} d\theta \quad (3.24)$$

with  $r = |k|$  One can see that instead of integrating over an infinite space namely the real plane, we can reduce the exponential term to an integration from 0 to two pi which then happens to be in the same form as a first kind Bessel function. We replace the term in equation 3.24

$$J(x) = \int_0^{2\pi} r e^{ir|x|\cos(\theta)} d\theta \quad (3.25)$$

Which would allow equation 24 to become,

$$G(x) = \int_0^\infty r^2 e^{-r^2 \sigma^2} J(x) dr \quad (3.26)$$

So

$$\sqrt{\frac{d^2}{dx^2} + \frac{d^2}{dz^2}} f(x) = \int_{R^2} G(x-y) \hat{\phi}(y) d^2 y \quad (3.27)$$

Which is a convolution of G with some function where we showed (15) can be written as (20)

### 3.3.2 Wave Implementation

In the iWave model, the wave equation 3.9 is what we are trying to model. As shown in the previous section, we can get the change in height for every point in space from the wave equation. Thus to get the dynamics of the waves we must model it numerically. From the previous section, the spatial gradient can be rewritten as a convolution of a kernel function and the surface. One can also discretize the temporal component through commonly used differencing methods. Therefore we can use numerical methods to discretize the wave equation and solve it for the surface.

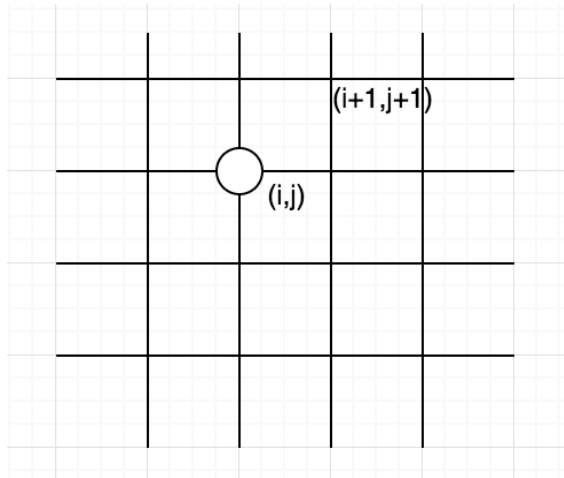


**Figure 3.8:** Illustration of how a vertex on the lattice,  $i,j$  are related to neighbouring points on the lattice which shows increasing  $i, j$  to the right and up respectively. The scale is determined through convenience, in my experiment, a scale of 0.1m is used

The first step would be to discretize the surface into a grid of vertex points  $i, j$  in the same fashion as figure 3.8. For each point on the grid our height function,  $h$ , would have some height at position  $i, j$ . With this notation, we can find the dynamics just by following the wave equation.

To discretize the 2d-convolution operator we note that the discrete convolution is

written as

$$\int_{R^2} G(x-y)\hat{\phi}(y)d^2y = \sum_{k=-P}^P \sum_{l=-P}^P G(k,l)h(i+k,j+l) \quad (3.28)$$

where  $P$  is the radius of influence and the sum goes for  $k$  and  $l$ . Since  $P$  is finite, a reasonable number should be chosen for the influence of the kernel. At farther positions the kernel has little effect, so we can keep  $P$  to be small and centered around  $i$  and  $j$ . For the kernel function  $G$ , since  $k$  and  $l$  are dependant on the size of  $P$ ,  $G$  can be pre-computed and stored in memory ahead of time.

$$G(k,l) = \sum_n q_n^2 e^{-\sigma q_n^2} J_0(q_n R_{kl}) / G_0 \quad (3.29)$$

Where  $R_{kl}$  is the radial distance,  $R = \sqrt{k^2 + l^2}$  and  $G_0$  is a scaling factor. It should be noted that  $q_n$  is the grid step size of the lattice, figure 3.8, with  $n$  being number of steps in the spatial grid discretization. So  $q_n$  in equation 3.29 replaces  $r$  in 3.28, in the equation above. Where  $q_n = n\Delta q$

Once the spatial gradient has been discretized, then it can be used to solve the second order differential equation. Since we have a second derivative and a first derivative, we use symmetric differencing for the second derivative portion and forward differencing for the first derivative. Thus for the temporal update we would compute

$$h(i,j,\Delta t) = h(i,j,t) \frac{2 - \alpha\Delta t}{1 + \alpha\Delta t} - h(i,j,t - \Delta t) \frac{1}{1 + \alpha\Delta t} - \frac{g\Delta t^2}{1 + \alpha\Delta t} \sum_{k=-P}^P \sum_{l=-P}^P G(k,l)h(i+k,j+l,t) \quad (3.30)$$

Thus, an explicit discretization of the wave equation, where  $\alpha$  is the damping factor

and  $g$  is gravity, can be implemented easily given that the convolution kernel is precomputed and uses a look-up operation when it is needed. In our experiments, this method was implemented by (Nordeus, Erik, 2018).

# Chapter 4

## Experiments and Results

In this study, I investigated which factors affect human perception of virtual liquids in augmented reality. I focused on three factors: (1) the dynamics of the liquid, (2) the surface texture/color of the texture and (3) the physical lighting in the room.

### 4.1 Hypotheses

#### **Hypothesis One:**

I am interested in whether users have a preference for one dynamic model over the other when comparing the fluid motion. I hypothesize that users will prefer the higher fidelity model, which in our case it would be iWave. I predict the effects from dynamics may be weaker in the presence of a more relatable object like the fake caustic texture and not depend on lighting.

**Hypothesis Two:**

I am interested in whether users have a preference for one texture of liquid over the other when comparing realism. I hypothesize that users will prefer the fake caustic texture over the plain texture. I predict that the effect from texture may be notably weaker in the presence of a smoother dynamic model and not depend on lighting.

**Hypothesis Three:**

I am interested in whether users have a preference for a certain real-world lighting environment overall regardless of other factors. I hypothesize that users will prefer the local lighting over the ambient lighting, since the virtual object was directly lit. I predict the effect from texture and dynamics on preferred lighting will be negligible regardless of presence of different textures or dynamics.

## 4.2 Methods

To answer which factor has the largest impact on perception in AR, I made a liquid object interaction animation. Specifically, a virtual ball drops from some height then impacts the simulated liquid. The user observed the interaction and the waves formed from the impact. The user was instructed to move their head so they could have different viewpoints of the interaction. The base environment we have is a virtual pool of liquid and an object interacting with the liquid. The virtual pool is presented in the environment on top of a real image target which is illustrated in figure 4.1. The ball repeated drops at a random location every time. The animation stimuli is shown in figure 4.5 and figure 4.6

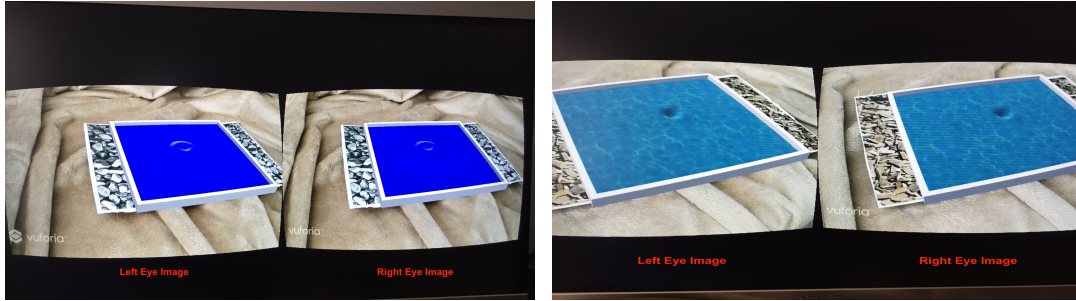


**Figure 4.1:** Demonstration of the user's view through the head-mounted display. The left is a simulation using a plain surface with wave particles. The right is a water texture surface simulated with iWave. Each image shows the left eye and right eye view which would be seen separately by each eye through the HMD optics.

To implement liquid-object interaction, the Unity game engine was used. Unity 2017 (Unity Technologies, 2018) is a freely available game engine, with paid extra features, that abstracts basic game components such as movement, physics, UI and objects and allows the user to focus on building a game or an interaction. Unity implements a wide range of physics which includes basics like gravity for falling objects to more complex interactions such as illumination of virtual objects with various algorithms. This capacity along with rapid prototyping, the abundance of external documentation and ready-made code made Unity a suitable choice. For example, iWave was already implemented (Nordeus, Erik, 2018) and I modified it to fit my requirements.

To create the virtual liquid, we used the Wave Particle method and iWave as discussed in Chapter 3. Since the iWave method uses grids to determine the height of the waves and wave particles deviate a surface, a flat surface object with a grid represents the undisturbed virtual liquid. Since a surface was used, simulating a liquid-object interaction can be reduced to deviating the vertex positions of the surface. This is

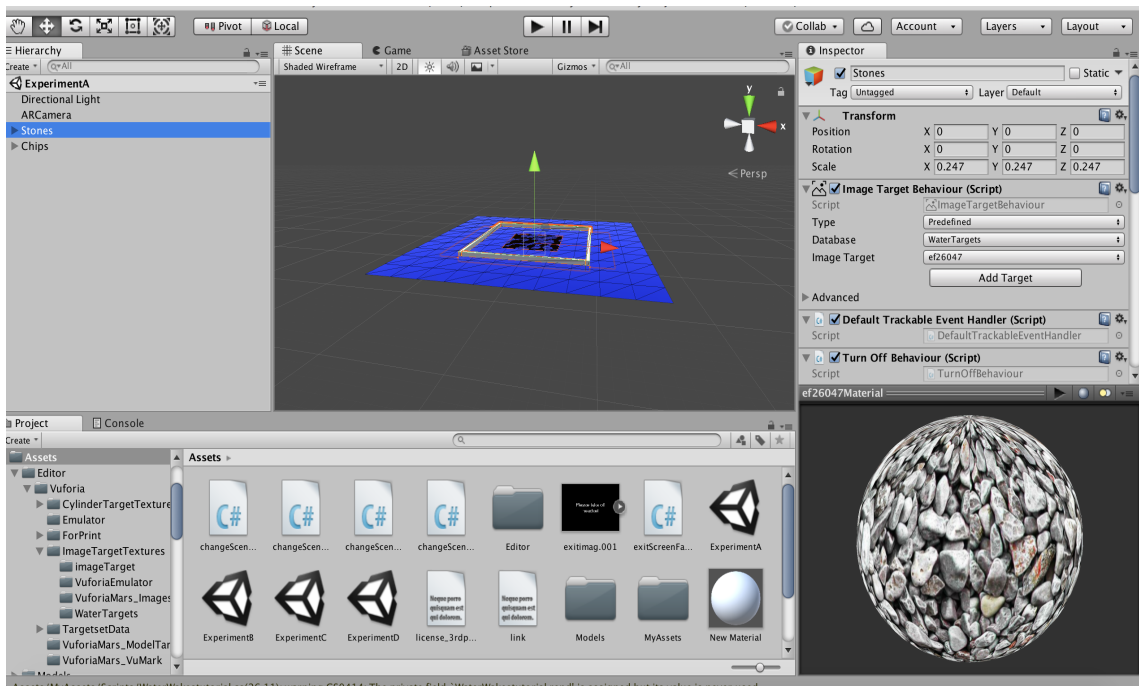


**Figure 4.2:** This demonstrates the development environment of unity and how it is used to create the liquid simulations.

a technique that is used by many other systems such as those detailed in (Nordeus, Erik, 2018) as well as a simple simulation of fluid using pipes (Mei, Decaudin, & Hu, 2007).

To enable real world augmentation, i.e. to add the virtual pool to the real world, Vuforia was the chosen experiment framework. Vuforia is a tool that tracks a custom image and overlays the virtual object on top of it which results in real world augmentation. It is noted that for tracking to be stable, a good image with a lot of natural feature points had to be used thus the two textures shown in the figure 4.3, above, were used as image targets. This was because they have a reasonably high number of feature points. Since Vuforia tracks the image targets, Vuforia is able to augment the real world such that the virtual object is in stereo while providing the video feed. Due

to the limitations of the hardware, the video feed was only taken from one camera rather than two cameras hence the video feed was not in stereo. (Vuforia, 2018).



**Figure 4.3:** These are the two image targets chosen for the experiment which are used for Unity to augment. They were chosen since they have good natural features to track as defined by Vuforia. The image on the left is named stones and the image on the right is named chips.

The most recent Android phone (a Google Pixel 2 XL)(Google, 2018c) available at the writing of this thesis was used. A mobile device was chosen since they are an important market for augmented reality applications. Another advantage to using a base Google device is that Unity and Vuforia are easily integrated into the software and the hardware. Since the phone is a Google device, integrating Google Cardboard, the head mounted application for their VR applications, was easy as well. Since the user is required to move their head around, the phone was attached to VR Box virtual reality glasses by VR box (VRBox, 2018).

### Stimuli Details

The stimuli consisted of a small pool of liquid that was displayed on top of the augmentation target. The pool of liquid was bounded by a square white border. After two seconds, a ball fell and hit the surface causing a wave. The ball would sink through. This was repeated every two seconds with the ball falling and striking



**Figure 4.4:** These were the Head mounted display, VR box, as well as the phone, Google Pixel 2, that were used to conduct the experiment. The pixel phone is inserted in the VR box and the screen was used to display an augmented image of the world to the wearer of the headset.

another location in the pool at random. These interactions can be illustrated in figure 4.5 and figure 4.6.

Since I am studying three factors, there are two different settings that are related to each factor. Two of the factors I am studying are related to the virtual stimuli namely be the dynamics and the texture of the liquid. These conditions will be referred to as virtual conditions. For the dynamics factor the two settings were, iWave and wave particle. In the simulation, as expected, it was found that iWave was smoother than the wave particle. For the texture settings, two variants were used, a plain blue texture and a fake caustic texture, shown in the left and right image respectively in figure 4.1. A fake caustic texture was used to emulate the look of a pool of water. Real caustics were not used since simulating these requires information about the environmental lighting and it is also computationally complex which would make the system harder to implement. As for the lighting factor, the settings are an



**Figure 4.5:** This demonstrates the stimuli through multiple frames and what they would see through. The wave model used in this demonstration is the iWave model. The texture on the object is the plain texture.

ambient lighting and a local lighting which is illustrated in figure 4.8. The choice of lighting was chosen because those two types were closest to how the virtual object was lit with the virtual lighting namely a lighting source right above the virtual object.

### 4.3 Experimental Design

I wish to answer the overarching question of which factors play a role in perceiving believability of virtual liquids in augmented reality. Thus to assess this question, I constructed the following experiment. I gave a comparison task to the user in which the users would compare between two stimuli as detailed before. Then they would be asked questions about what they saw.

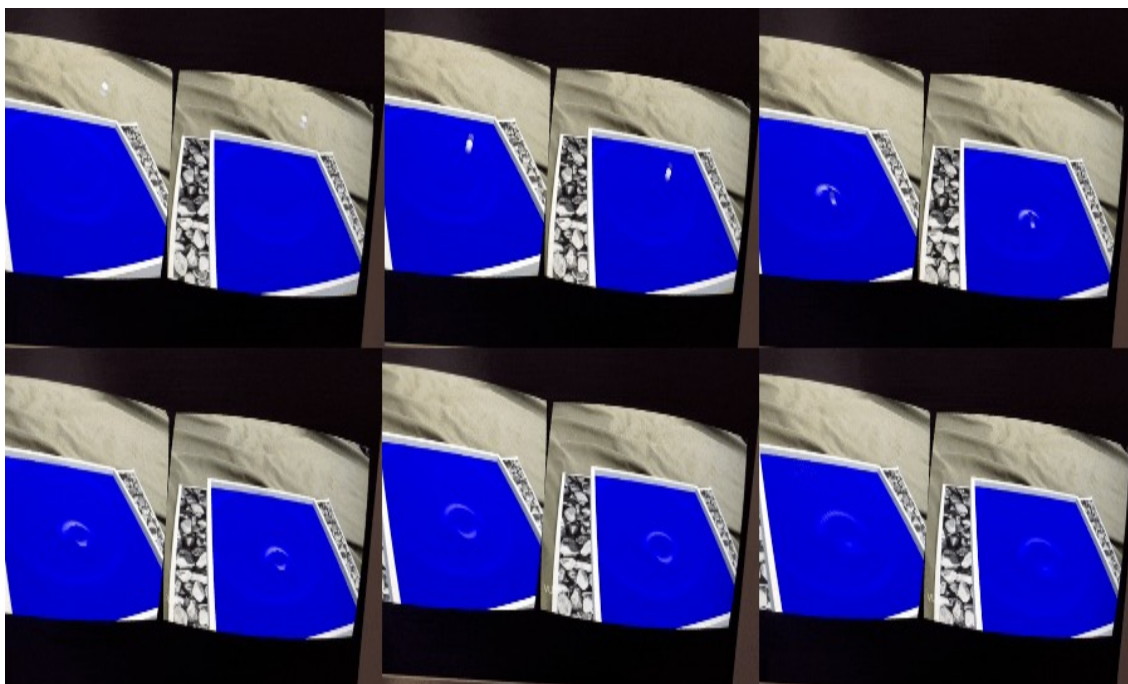


**Figure 4.6:** This demonstrates the stimuli through multiple frames and what they would see through. The wave model used in this demonstration is the wave particle model. The texture on the object is the plain texture.

### 4.3.1 Environment and Procedure

The participant was placed between the two image targets, as shown in in figure 4.3, one to their left and one to their right. On each side, they could see the image target for augmentation, a light source and a green Lego brick. The rest of the environment was covered with a black backdrop as shown in figure 4.7. The Lego brick was placed to ensure that the user was aware that they were in a real environment, by giving a cue to the environmental lighting, and not a pure virtual environment. It was also used to see if peripheral items would be a distraction however, upon discussion with the participants after the study all of them reported not to have noticed the brick during the sessions.

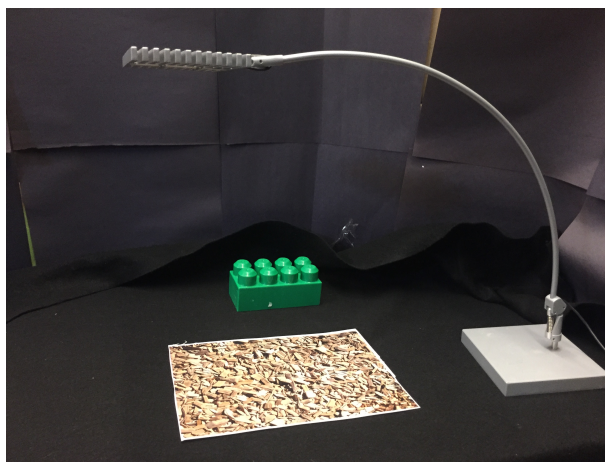


**Figure 4.7:** This is the scene that the user looked at through the head mounted display. The image target is placed in the center with a light source above it as well as a green brick as possible distraction in the peripheral.

After being placed, the participant was instructed to look either to their right or their left first then look at the opposing side. The participant, once seeing the augmentation, inspected the scene and moved their head and/or body around to have different vantage points to observe the interaction. While they were looking at the stimuli, the participant was asked three questions verbally and their responses recorded. Afterwards, the lighting environment was be changed and the same instructions were followed, namely moving their heads and being asked the same questions. At the end of the task, a fourth question was asked in which they compared the two lighting conditions separately for both the left and right augmentation.

Since the participants were doing comparisons, conditions were blocked into pairs comparing: (1) stimuli with different dynamics but the same texture and (2) stimuli with different texture but the same dynamics. For each block, the pair was first compared under one lighting condition then the other lighting condition, the order of which was randomly determined. Finally each of the right and left stimuli were

compared between the two lighting conditions. Each block is detailed in in table 4.1 while the flow of this experiment is outlined in figure 4.9.

To ensure that there was no bias from the order in which the stimuli were presented, all the participants viewed the same pairs but in different order for each participant. Each participant was given a random order such that every even pair in the order started with local light then ambient light while every odd pair was reversed. Each left and right image target would vary between participants and thus during the analysis responses were normalized to present data in the same order for all the comparisons between a pair of conditions. This ensured that order of presentation of both comparisons and lighting were randomized across subjects. For this study, we took participants from the lab as well as a few external participants. The age range was from 19 to 32 with 8 males and 4 females. All of the users were students attending York University, some were members of the same lab as the experimenter. All participants could see clearly either unaided or with their habitual corrective glasses. Users were also able to adjust the focus and interpupillary distance of the headset to ensure what they saw was clear.

### **4.3.2 Questions**

To facilitate analyzing the effect of each factor, four statements were asked which were then mapped to a Likert scale indicating a preference between two stimulus conditions. The statements are as follows

1. The result of the initial ball impact looked more realistic in the left image than in the right image

2. The waves after the ball interaction looked more realistic in the left image than in to the right image
3. The surface of the left surface looked more realistic then the right image
4. The first lighting condition was preferred over the second for image on the (left/right)

To answer these statements, questions were asked pertaining to each statement in two parts. For example, for the side preference questions, first the viewer was asked which side they preferred, left or right based on the qualities of the statement. Then a follow up question was asked to see to what degree they preferred this side. Responses were translated to a Likert scale where 1 indicated that they strongly preferred the right virtual object to 5 indicating that they strongly preferred the left object, with 2 and 4 being their respective slightly prefer responses and 3 indicated neither preferred or a neutral response to answer the above statements. This turns the response to a comparison ordinal rather than a standard Likert response.

For the statements above, each statement mainly addresses one of the factors being studied with questions one and two referring to the dynamics, question three referring to the texture and question four referring to the room lighting. Statements one to three were asked for each block of stimuli. Since statement four is about the lighting, it was only asked when the user had already viewed both lighting conditions and for a fixed set of virtual conditions.

For the rest of the chapter, to simplify, I will refer to the settings of the factors by the following notation as specified in table 4.1.

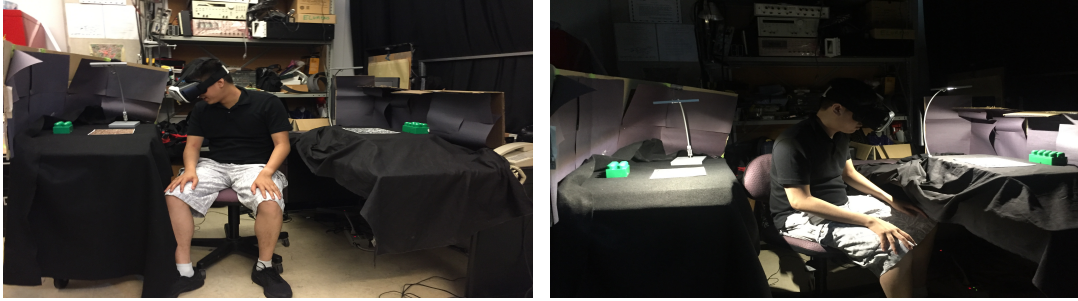


**Figure 4.8:** Both these images convey two things, they demonstrate how the experiment was done. The user was placed in between two setups and looked between the two. The image on the left demonstrates how the environment looked like for ambient lighting while the image on the right demonstrates how the environment was lit for the local lighting.

| Factor setting notation |                      |       |
|-------------------------|----------------------|-------|
| Symbol                  | Setting Name         | $x_i$ |
| $T_1$                   | Fake Caustic Texture | 1     |
| $T_2$                   | Plain Texture        | -1    |
| $D_1$                   | Water Particle       | 1     |
| $D_2$                   | iWave                | -1    |
| $L_1$                   | Ambient Lighting     | 1     |
| $L_2$                   | Local Lighting       | -1    |

**Table 4.1:** The notation used to label the different conditions of the experiment. The first column is the symbol corresponding to the condition, the second column while the third column is the x value assigned for that setting which would be used in the data analysis

## 4.4 Data Analysis

In our experiments two virtual objects with various settings were compared and, table 4.2 and 4.3 show all comparisons that were done.

### 4.4.1 Data

The data collected were the responses to the questions mapped to a 5 point Likert scale ranging from strongly prefer the left, slightly prefer the left image, neutral,

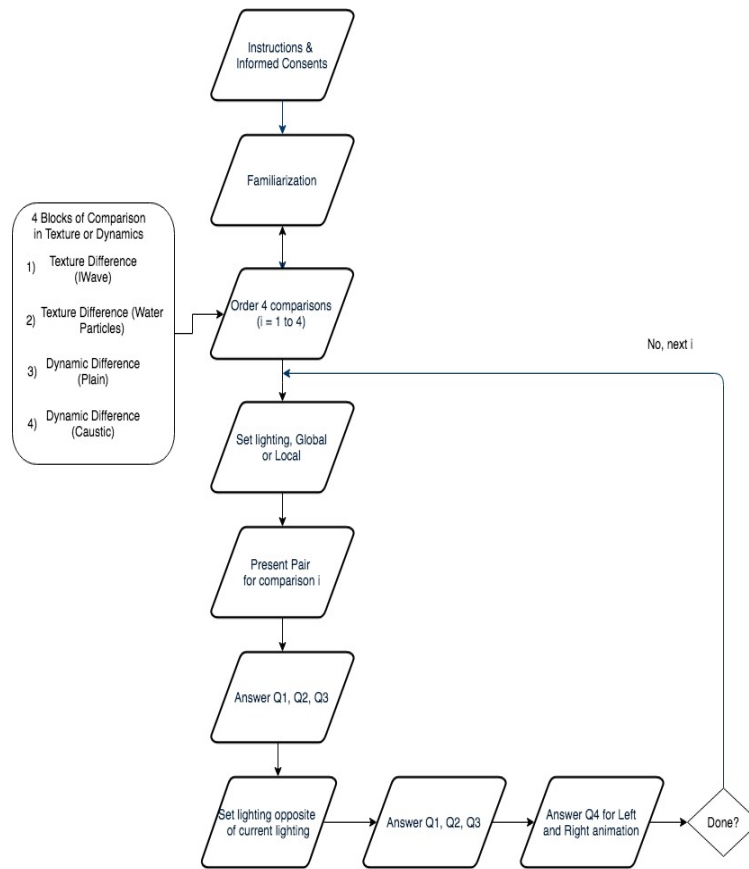


**Figure 4.9:** This flow chart demonstrates the whole procedure of the experiment from what pair of stimuli were presented to the order in which the pairs were presented and the questions that were asked at a stage during the experiment

slightly prefer the right, and strongly prefer the right image. All pairs were presented in both orders (Condition 1 on the left, 2 on the right and condition 1 on the right , 2 on the left) and the data transformed to indicate preferred for each condition not side. All the comparisons are presented on the data labels on the histograms, so for  $D_2$  vs  $D_1$ , that means  $D_2$  is preferred to the left and  $D_1$  is preferred to the right. The data shown below in figures 4.10 to 4.13 are the histograms of the data collected for each question and each setting.

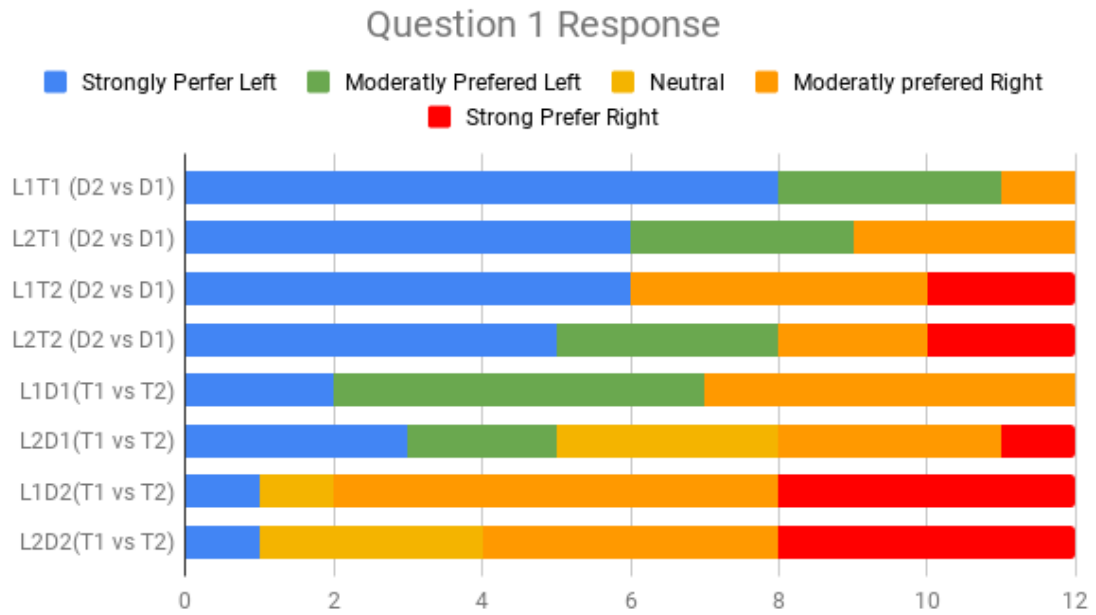


**Figure 4.10:** The responses from questions 1 for both dynamic and texture comparisons. Question one was "The result of the initial ball interaction looked more realistic in the left image than in the right image"

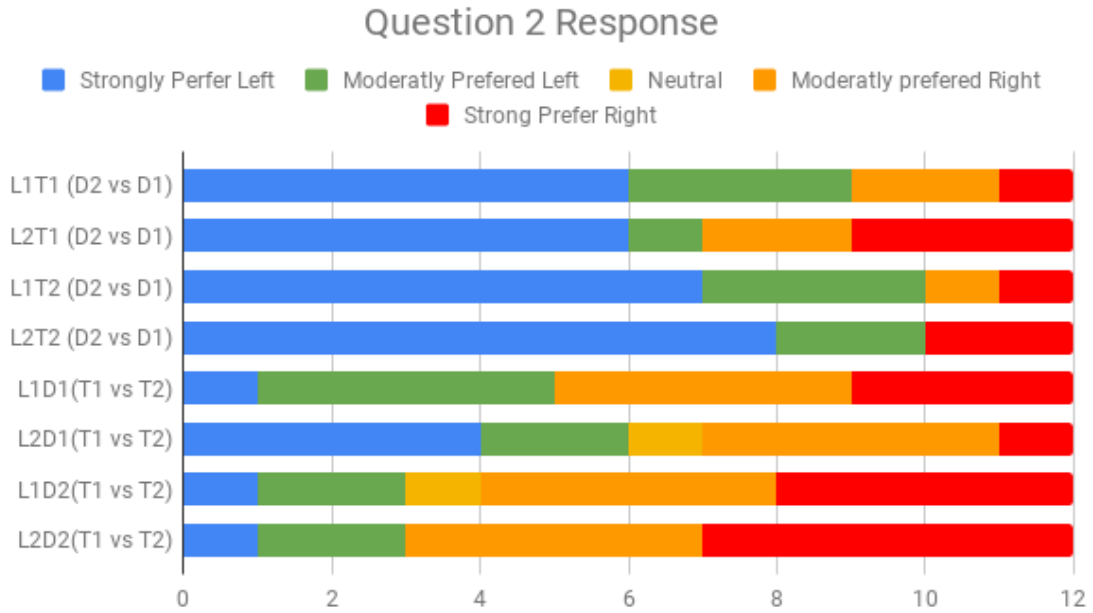


**Figure 4.11:** The responses from questions 2 for both dynamic and texture comparisons. Question 2 was "The waves after the ball interaction looked more realistic in the left image than in to the right image"

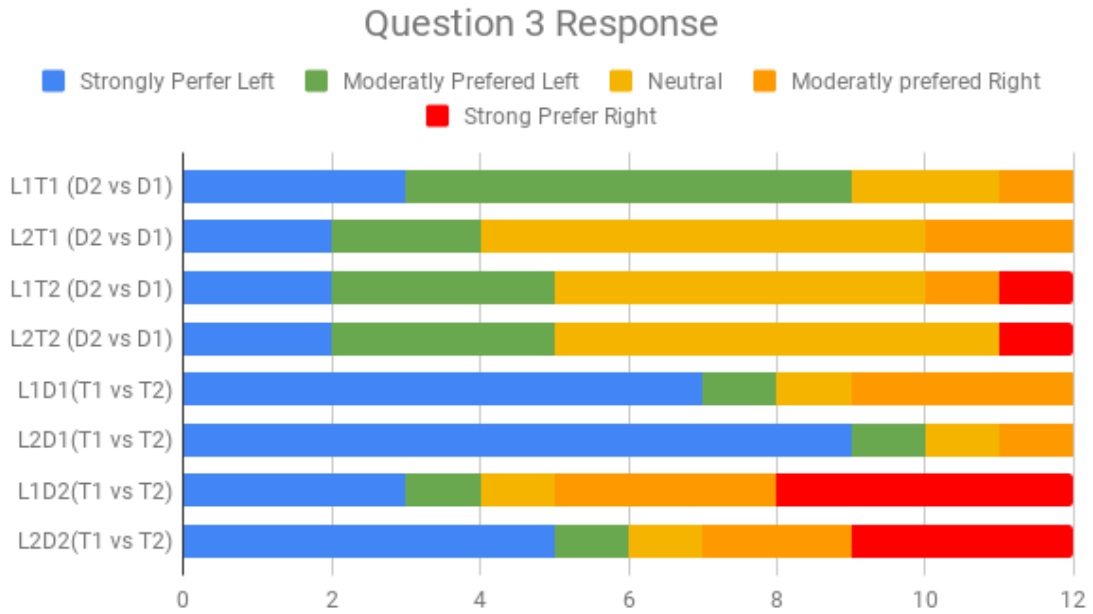


**Figure 4.12:** The responses from questions 3 for both dynamic and texture comparisons. Question 3 was "The surface of the left surface looked more realistic relative to the right image"

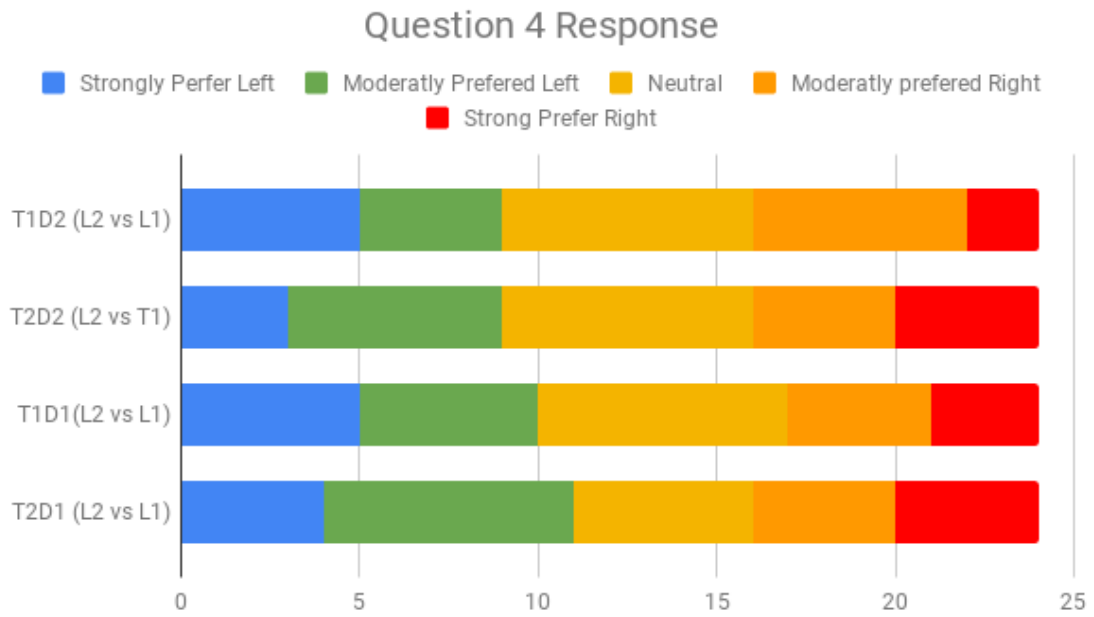


**Figure 4.13:** The responses from questions 4 for all settings. Question 4 was "The local light was preferred over the ambient light for the image on the (left/right)"

| List of Comparisons where Q1 to Q3 Were asked        |             |             |
|--|-------------|-------------|
| Pairs differing in dynamics (other factors constant) | $L_1T_1D_1$ | $L_1T_1D_2$ |
|  | $L_2T_1D_1$ | $L_2T_1D_2$ |
|  | $L_1T_2D_1$ | $L_1T_2D_2$ |
|  | $L_2T_2D_1$ | $L_2T_2D_2$ |
| Pairs differing in texture (other factors constant)  | $L_1T_1D_1$ | $L_1T_2D_1$ |
|  | $L_2T_1D_1$ | $L_2T_2D_1$ |
|  | $L_1T_2D_2$ | $L_1T_1D_2$ |
|  | $L_2T_2D_2$ | $L_2T_1D_2$ |

**Table 4.2:** The pairs that were used for question 1 to 3 the dynamic and texture questions

| List of Comparisons where Q4 was asked |             |
|--|-------------|
| $L_1T_1D_1$                            | $L_2T_1D_1$ |
| $L_1T_1D_2$                            | $L_2T_1D_2$ |
| $L_1T_2D_1$                            | $L_2T_2D_1$ |
| $L_1T_2D_2$                            | $L_2T_1D_2$ |

**Table 4.3:** The pairs that were used for question 4 the lighting question

## 4.4.2 Analysis

### Analysis Techniques

To determine the effects of the factors in the perception of the liquid object interaction in our experiments, we did the following analysis. Analysis was performed using the statistical software R except for one Wilcoxon test computed using Excel.

Since the data obtained was in a Likert form comparing pairs of conditions, an extension of the Bradley-Terry-Luce model was used to model the response through a cumulative link model (CLM) with symmetry conditioning on the thresholds (Agresti, 1992). The reason for this is to have a comparable measure of how the response to

each question was affected by each factor. In the model equation 4.1,  $Y_{r,l}$  refers to the response of a question comparing the left side to the right side (Casalicchio, 2013) where what was left and what was right is illustrated in table 4.2 where a higher value indicated a preference for the left and a lower value indicated a preference for the right. It is of note that the CLM model was used to model the response for questions 1 to 3 since there were enough comparisons to create the model. The CLM model is used to find  $\gamma(x_l, x_t, x_d)$  for a fixed input of factor setting values

$$\begin{aligned} \text{logit}(P(Y_{l,r} < k | (l, r))) = & \theta_k + x_1\gamma(L_1, T_1, D_1) + x_2\gamma(L_1, T_2, D_1) \\ & + x_3\gamma(L_1, T_1, D_2) + x_4\gamma(L_1, T_2, D_2) \end{aligned} \quad (4.1)$$

with  $k$  going from one to four.

Since CLM models  $\gamma(x_l, x_t, x_d)$  for a fixed input, i.e.  $\gamma(L_1, T_1, D_1)$  rather than individual contributions from factors then from (Taneva, Giesen, Zolliker, & Mueller, 2009), I model the contribution from each factor by modeling  $\gamma(x_l, x_t, x_d)$ . To do this, I model  $\gamma(x_l, x_t, x_d)$  through a linear model in equation 4.2. The independent variables for lighting, dynamics and texture,  $x_l$ ,  $x_d$  and  $x_t$  were encoded with a value of -1 or 1, as in table 4.1. Thus to model the effects from the responses for each question, the model is written as

$$\gamma(x_l, x_t, x_d) = Lx_l + Dx_d + Tx_t + b \quad (4.2)$$

where  $L$  is the contribution from lighting,  $D$  is the contribution from the dynamics and  $T$  is the contribution from the texture and with  $b$  a bias term.

Since for questions 1 to 3,  $L_1$  was not compared to  $L_2$ , then there were not enough comparisons to create one CLM model. Hence, two CLMs corresponding to equation 4.1, were constructed with one for  $L_1$ , the ambient lighting and the other for  $L_2$ , the local lighting.

To find the coefficient for the interaction values from the CLM model detailed in (Agresti, 1992), I used ordBTL from (Casalicchio, 2013), which is available as an R routine that can compute the CLM with the symmetry condition for comparison ordinal data. This gives the  $\gamma(x_l, x_t, x_d)$  for fixed inputs. Now the task would be to model the  $\gamma(x_l, x_t, x_d)$  to find out which factor is important in answering each of the questions. To find L, D and T that would model  $\gamma(x_l, x_t, x_d)$ , I have an over-determined system of equations (i.e. I would have 8 equations, one for each time question one to three was asked, and four unknowns for each question one to three). Thus to approximate L, D and T I use ordinary least square which would give me an approximate L, D, T and b for my over-determined system. The results of this analysis are shown in table 4.4

| Coefficients to Linear Model |                          |        |        |                          |
|------------------------------|--------------------------|--------|--------|--------------------------|
|                              | L                        | D      | T      | b                        |
| Question 1                   | 0.000                    | -0.659 | -0.165 | 0.000                    |
| Question 2                   | $-4.163 \times 10^{-17}$ | -0.649 | -0.205 | $-1.380 \times 10^{-17}$ |
| Question 3                   | 0.000                    | -0.290 | 0.495  | 0.000                    |

**Table 4.4:** The coefficients that were estimated from the CLM model that for each factor in the linear model of the responses for questions one to three

In the table 4.4, above, to determine how significant the coefficients are two tests must be conducted. One is to see if the results from the CLM are significant. This means that the p value calculated from the residual deviance is statistically significant

which, for our case, shows that the data is a good fit. Second, to determine if the linear model, equation 4.2 was adequate, a coefficient of determination was computed with higher values indicating a better fit. For the models computed, the residual degrees of freedom was 11. For question 1, the coefficients were significant ( $p < 0.01$ ) and had a coefficient of determination of 0.963. For question 2, the coefficients were significant ( $p < 0.05$ ) and had a coefficient of determination of 0.879. For question 3, the coefficients were significant ( $p < 0.0025$ ) and had a coefficient of determination of 0.776.

### **Preference for dynamics in the interaction and wave motion**

I expected the effects of the dynamics to be mainly evident in questions 1 and 2 since they were about the dynamics of the system. Question 1 asked about the initial impact while question 2 asked about the waves after the impact. For these questions, a choice between two settings of the virtual object were displayed, following table 4.2. If hypothesis 1 is true, then the higher fidelity model should be preferred which is  $D_2$ .

In determining which dynamics model was preferred overall I wanted to test the median of the responses to questions 1 and question 2 for the dynamic comparisons only, and determine if they were statistically significantly different from a neutral response. To achieve this, I conducted a one-sample Wilcoxon signed rank test in which I took the responses for questions one and two for the dynamic comparisons, averaged them and subtracted the data by 3 to obtain a signed value. The hypotheses for the Wilcoxon signed rank test are satisfied since the pair comes from one participant (paired differences), each participant is independent and the data collected is ordinal

in nature. Then I did the Wilcoxon signed rank test on these new values to find if I could reject the hypothesis that the median of the data was 3, which is a neutral response. I also determined which dynamics was preferred,  $D_1$  or  $D_2$  by taking the median of the average of the response subtracted by 3. If the value was negative then that implies  $D_2$  was preferred and if the value was positive then  $D_1$  was preferred.

Looking at table 4.5, indicates that the p values are indeed small but only the case of  $L_1T_1$  has a p value small enough to be statistically significant ( $p = 0.008$ ). Since I have four comparisons, after doing a Bonferroni correction, the p-value must be lower than 0.0125 for statistical significance rather than 0.05. Thus the preference bias for the other settings,  $L_2T_1$ ,  $L_1T_2$ , and  $L_2T_2$  were not statistically significant. It should be noted that all the medians are negative indicating that  $D_2$  is indeed preferred overall.

In determining the effect from the other factors on the dynamic preference, the CLM described in the analysis technique section was used. Table 4.4, from before, shows the dynamics coefficient was the largest for both of these questions (in absolute value). There were also non-zero effects of L and T on those questions as well but the coefficients were smaller. That is in Table 4.4, for question 1, the D value was 0.659 while the T value was 0.165 while for questions 2, D had a value of 0.649 and T had a smaller value of 0.205 (all in absolute values). As expected, the dynamics had the largest role in the dynamics based questions but T had a non-zero role. In question one, L had a value of zero while in question two it had a very small coefficient value not significantly different from zero. This indicates that lighting did not have an effect on the decisions of which dynamics were preferred.

| Wilcoxon test values for testing for the median of the average of questions 1 and 2 for Dynamics Comparison Task |          |          |          |          |
|--|----------|----------|----------|----------|
|  | $L_1T_1$ | $L_1T_2$ | $L_2T_1$ | $L_2T_2$ |
| p-value  | 0.008    | 0.066    | 0.086    | 0.146    |
| Median   | -2.00    | -0.63    | -1.19    | -1.50    |

**Table 4.5:** The results when testing if the median of the response is statistically significant from 3. The criterion p-value was 0.0125 after a Bonferroni Correction. The median is based on the ranked response of the average of questions 1 and 2 subtracted by a constant of 3.0 to centre the results at a neutral response

### Preference for Realism

Question 3 focused on the realistic appearance of the water surface which includes the coloring of the surface as well as the surface appearance. The settings that were being compared are outlined in Table 4.2 in which question three was asked for those comparisons. If hypothesis 2 is true, then users should have preferred a fake caustic texturing rather than a plain texturing.

In determining which texture was preferred overall I wanted to see what was the median response to question 3 for the texture comparison conditions only and whether it was statistically significant from a neutral mean. To achieve this, I conducted a one-sample Wilcoxon test in which I took the responses for question 3 and subtracted 3 from the data to obtain a signed value. The Wilcoxon assumptions were satisfied with the same reasoning as in the dynamics. Then I did a Wilcoxon signed test to see if I could reject that the median was statistically significant from 3, which is a neutral response. I also determined which texture was preferred,  $T_1$  or  $T_2$  by taking the median of the response subtracted by 3. If the value was negative then that implies  $T_1$  is preferred and if the value was positive then  $T_2$  was preferred.

As shown in table 4.6 the p values for when the dynamics was  $D_1$  were less than 0.05 from which I could reject that the median was three. It should be noted that since we have four comparisons, after a Bonferroni correction, the p value that must be met for significance would be 0.0125 which implies that the  $L_1D_1$  was not significant but  $L_2D_1$  still was. It should be noted that the median is negative for  $D_1$  but close to zero for  $D_2$  which implies a preference for the fake caustic texture for the wave particle model but not necessarily in the iWave model. This indicates an effect from the dynamics when people consider realness of the surface and not just the surface texture.

| Wilcoxon test values for testing the median of question 3 for Texture Comparison Task |          |          |                 |                   |
|---|----------|----------|-----------------|-------------------|
|   | $L_1D_1$ | $L_2D_1$ | $L_1D_2$        | $L_2D_2$          |
| p-value   | 0.019    | 0.003    | 0.550           | 0.5453            |
| Median  | -1.5     | -2.0     | $1.1 * 10^{-5}$ | $-4.78 * 10^{-3}$ |

**Table 4.6:** The results of testing if the median responses is statistically significantly different from 3. The criterion p-value was 0.0125 after a Bonferroni Correction the ranked response of question 3 subtracted by by a constant of 3.0 to centre the results to a neutral response

In determining the extent of how much the other factors affected the choice of realism of the surface, I looked at the CLM model for question 3 in which the model was explained in the analysis technique section and in table 4.4 above. As predicted, texture had the largest effect since the value for T in table 4.4 was 0.4. Table 4.4 shows that the contribution from the dynamics was only about half of the contribution from the texture. This indicates, that when doing comparisons on texture, the participants also factored the dynamics when responding to question 3. This indicates that not only the texture was used for realism of the surface. As observed, L was 0 for question

three which suggests that lighting also did not have a role when determining question 3.

### **Preference for Lighting**

Participants were asked lighting preferences for each combination of virtual factor settings, dynamics and texture, as outlined in table 4.3. If hypothesis 3 is true then they would prefer local lighting.

To determine which lighting was preferred I tested whether the median of the responses from question four was statistically significantly different from a neutral response. To achieve this, I conducted a one-sample Wilcoxon test in which I took the responses, subtracted them by 3 to find the signed values. Then to determine which lighting was preferred,  $L_1$  or  $L_2$ , I took the median of the response. If the median value was negative then  $L_1$  was preferred if the median value was positive then  $L_2$  was preferred.

When looking at table 4.7, all p values are significantly greater than the 0.05 threshold. Along with all median values being close to zero, within 5 significant digits at least, this implies that hypothesis three was not satisfied since the p values and other values indicate that the median for the lighting is in fact three.

To determine if texture or dynamics had an effect on the choice of lighting conditions, I compared the responses from question 4 for pairs of conditions. For example, I compared the response value on question four from settings with  $D_1$  and subtracting the value of the same questions with a setting value  $D_2$ , such that the texture, T, was the same. As shown in table 4.8, the z-score from a two sample Wilcoxon signed rank

| Wilcoxon test values for testing for the median of responses for questions 4 for Lighting Comparison Task |                 |                  |                 |          |
|---|-----------------|------------------|-----------------|----------|
|   | $T_1D_1$        | $T_2D_1$         | $T_1D_2$        | $T_1D_2$ |
| p-value   | 0.4487          | 0.9416           | 0.4354          | 0.5      |
| Median Rank   | $-5.92*10^{-6}$ | $4.01 * 10^{-6}$ | $-4.62*10^{-5}$ | 0        |

**Table 4.7:** The results when checking if the median of the responses was statistically significant from a median of 3. The ranked median generated from the response of question 4 subtracted by a constant of 3.0 to centre the results to a neutral response

test was not above the 95% critical value of 1.96. This means that there is no effect from dynamics in the preference of lighting. There was also no statistical significant effect of texture on the choice of lighting model. This is observed in table 4.8 for settings  $T_1 - T_2$  where the z-score values were less than than the critical value of 1.96.

| Wilcoxon Test for Question 4 |                  |                  |                  |                  |
|------------------------------|------------------|------------------|------------------|------------------|
| Shared Factor                | $T_1(D_1 - D_2)$ | $T_2(D_1 - D_2)$ | $D_1(T_1 - T_2)$ | $D_2(T_1 - T_2)$ |
| Z-score                      | -0.105           | 0.103            | -0.314           | -0.402           |

**Table 4.8:** The results when comparing the responses to question four for dynamics and texture. Since the test is ranked, a negative value would imply a stronger preference to the setting with the minus sign in front while a positive value would imply a stronger preference to the setting without the minus sign. Since this is a z-score, a value that would imply statistical significance is 1.96 or greater.

### 4.4.3 Discussion

What we have shown through the coefficients from the model in table 4.4 is that dynamics had a larger effect in texture based questions than the other way around. This can be demonstrated by the fact that when asking question 3 about the realism of the surface, the coefficient for dynamics was large in comparison to the coefficient

to the texture. This is in agreement with the work by (van Assen & Fleming, 2016) in which the skinning of the texture did not have an effect on people's perception in liquid simulations. This thesis extends this conclusion to object-liquid interaction in AR.

For hypothesis one, I found evidence that the preferred dynamics are indeed the high fidelity one. It has also been shown that the dynamics had an effect on texture judgments by first the coefficients being about half of the texture component as well as a large difference of p-values when changing between the dynamics.

For hypothesis two, the preference of  $T_1$  was shown only for the case of  $D_1$ . When  $D_2$  was used, there was no clear preference since the median was close to 0 and also the p-values were much larger than the 0.05 threshold. It should be noted that  $L_2D_1$  has a p-value for the texture effect less than the Bonferroni threshold of 0.0125. This is of interest because there were two participants who preferred  $T_2$  in the ambient lighting case but switched their minds to  $T_1$  in the local lighting case. As for how texture affects judgement of dynamics, there is some effects evident from the CLM but not to the extent that dynamics had on realism.

For hypothesis three, the preference is definitely neutral since all p values were greater than 0.05. This indicates that the choice of lighting does not matter since the participants felt neutral about it. Also from the CLM model, since the lighting coefficients were near zero, it seems to have no effect at all on the questions relating to other factors. It should be noted that having a neutral response was evident in the histogram of the question 4 as illustrated in figure 4.13 where the data centered on a mean of 3, yellow. It is of note that this result is consistent with the results from

(Knecht et al., 2011) in which lighting or shadows had no role in perception of depth in a augmented reality setting.

# Chapter 5

## Conclusion

### 5.1 Future Work

In this work, there were some experimental limitations as well as constraints on technologies and techniques. One of these concessions would be using a wave approximation rather than a full or close to full solver for the Navier-Stokes equations. Due to the speed in which these technologies evolve, a trivial extension of my work would be to use the latest AR devices and mobile phones on the market and repeat the experiment. Since the newest glasses have markerless AR built in, that is they do not require an image target, one could use them to see if similar results are acquired. The extent to how the additive nature of these augmentations would affect our study, namely fluids, is an avenue of research.

Another immediate extension would be to use different fluid models to do the comparison. One can use animations or other real time methods. Ideally, real time methods would be preferred due to the natural requirements for interaction in an

augmented reality. This would lead to exploring the use of other surface methods such as the extension of iWave by (Tessendorf, 2004). Other methods would include the ones described by (Mei et al., 2007) or an even following a different simplifications of the Navier-Stokes equation such shallow fluid equations (Chentanez & Müller, 2010). These methods would be of interest to compare with wave equation methods.

In the original thesis by (Yuksel, 2010), he outlined how to deal with objects that have buoyant forces. In our experiments we only had the objects that sank through the surface when hitting the surface, similar to a stone dropped in water. It is of interest to drop object with different physical properties such as objects that can float or sink then float. This would require some more work since the other objects being dropped would have to interact with not only the liquid but potentially other objects that are floating on the surface of the fluid.

In (van Assen & Fleming, 2016), they discussed extensively about the viscosity of liquids. Another extension could be to see if adding physical liquid properties as a factor would affect the perception of object-liquid interactions. Implementing viscosity with the wave equation would result in controlling the damping factor but if one would extend this by solving the Naiver-Stokes simplifications like in (Lee & O’Sullivan, 2007), then it would be more computationally intensive since in most real time liquid simulators viscosity is ignored. This is due to the fact that solving with viscosity adds another layer of complexity in the solver and may not be feasible to solve in real time i.e. at around 30 frames per second. It should be of note that a simpler physical property of liquid could be employed and compared namely ambient waves. In oceans, there are already ambient waves without any object interaction

on the surface. One could add ambient waves to the simulation and compare waves strengths to see if there is a difference, i.e. take it as a factor. One would assume that having ambient waves would increase the noise in the system thus noisier methods might perform better or there may be little difference between the methods, where cheaper methods would win out.

A important feature that was left out of our experiments was the addition of true light caustics due to the added complexity to the system. In my experiment, the fake caustic texture was used to give the user a feeling that what they were looking at was caustic water. However, since caustics are expensive to compute, more resources would have been required. It would be of interest since real environment lighting would definitely have an affect on the caustics of the virtual object. Thus one would have more to consider approximating the real world lighting which would then be translated into the virtual illumination. Since Unity does not have inherent support for modeling real world caustics system, a new light simulation system would had to implemented and integrated with the augmentation and liquid simulation.

One other avenue that was limited by the technology at the time was adding in real world interaction with either the hand or movement of the image target. This was briefly explored in the beginning, however it was found that the if one wanted to move the image target, finding how fast the image target moved, was too noisy. Future work might incorporate new sensors and/or software to enable participants to see how actually moving liquid and having it splash around would affect its realism.

## 5.2 Concluding Remarks

I have shown that out of the three factors, dynamics of the liquid object interaction is more important than the other two, surface skinning/texturing and real world lighting. This is reflected in the find that texturing had a negligible contribution on the dynamic judgments while the dynamic values had a comparable contribution to the texture in judgments of surface appearance results in the linear model equation 4.1 and 4.2. It was also shown that lighting had no effect as demonstrated by the coefficients being zero in the model for questions one to three. It is also of note that when comparing the distribution of the lighting preference, namely which lighting condition the user preferred, the mean was closest to a neutral response meaning, there was no preference between the two environmental lighting conditions since the differences were not statistically significant.

With these results in mind, some interesting applications could be found. If an application developer wants to create an experience they need not worry as much about how lighting would look in a scene. Even for local and ambient environmental lighting environments, there was not much of an effect on user preference. Thus if one were to create an application, they should focus their efforts on finding a very good liquid dynamic model. Overall, this work confirms results from computer graphics and introduces other avenues that one can research about for this new technology. This is only the beginning of liquid interactions in head mounted augmented reality with many more comparisons that can be done in the future.

# References

- Agresti, A. (1992). Analysis of Ordinal Paired Comparison Data. *Journal of the Royal Statistical Society. Series C. Applied Statistics*, 41(2), 287–297.
- Apple. (2018). ARKit. <https://developer.apple.com/arkit/>. Accessed: 2018-12-8.
- Bates, C., Battaglia, P. W., Yildirim, I., & Tenenbaum, J. B. (2015). Humans Predict Liquid Dynamics using Probabilistic Simulation. In *Proceedings of the 37th Annual Conference of the Cognitive Science Society* (pp. 172–177).
- Bojrab, M., Abdul-Massih, M., & Benes, B. (2013). Perceptual Importance of Lighting Phenomena in Rendering of Animated Water. *ACM Transactions on Applied Perception*, 10(1), 2:1–2:18.
- Brackbill, J. U., Kothe, D. B., & Ruppel, H. M. (1988). Flip: A Low-dissipation, Particle-in-cell Method for Fluid Flow. *Computer Physics Communications*, 48(1), 25–38.
- Bridson, R. (2015). *Fluid Simulation for Computer Graphics* (2nd Edition). CRC Press.
- Canabal, J. A., Miraut, D., Thuerey, N., Kim, T., Portilla, J., & Otaduy, M. A. (2016). Dispersion Kernels for Water Wave Simulation. *ACM Transactions on Graphics*, 35(6), 202:1–202:10.

- Casalicchio, G. (2013). *Modelling Comparison Data with Ordinal Response* (Doctoral dissertation, Ludwig-Maximilians-Universität München).
- Chentanez, N. & Müller, M. (2010). Real-time Simulation of Large Bodies of Water with Small Scale Details. In *Proceedings of the 2010 SIGGRAPH/Eurographics Symposium on Computer Animation* (pp. 197–206).
- Debevec, P. (1998). Rendering Synthetic Objects into Real Scenes : Bridging Traditional and Image-based Graphics with Global Illumination and High Dynamic Range Photography. In *Proceedings of the 25th Annual Conference on Computer graphics and Interactive Techniques* (pp. 189–198).
- Eriksson, K., Esterp, D., Hansbo, P., & Johnson, C. (1996). *Computational Differential Equations* (1st ed.). Cambridge University Press.
- Fleming, R., Wiebel, C., & Gegenfurtner, K. (2013). Perceptual Qualities and Material Classes. *Journal of Vision*, 13(8), 9–9.
- Gingold, R. A. & Monaghan, J. J. (1977). Smoothed particle hydrodynamics - Theory and Application to Non-spherical Stars. In *Monthly Notices of the Royal Astronomical Society* (Vol. 181, pp. 375–389).
- Google. (2018a). ARCore. <https://developers.google.com/ar/>. Accessed: 2018-12-9.
- Google. (2018b). Google Cardboard. <https://vr.google.com/cardboard/>. Accessed: 2018-12-9.
- Google. (2018c). Pixel 2. <https://store.google.com/product/pixel.2>. Accessed: 2018-12-16.
- Hattenberger, T. J., Fairchild, M. D., Johnson, G. M., & Salvaggio, C. (2009). A Psychophysical Investigation of Global Illumination Algorithms Used in Augmented Reality. *ACM Transactions on Applied Perception*, 6(1), 1–22.

- Kan, P., Dunser, A., Billinghamurst, M., Schonauer, C., & Kaufmann, H. (2014). The Effects of Direct and Global Illumination on Presence in Augmented Reality. In *Challenging Presence - Proceedings of 15th International Conference on Presence (ISPR 2014)* (pp. 223–230).
- Knecht, M., Dünser, A., Traxler, C., Wimmer, M., & Grasset, R. (2011). A Framework for Perceptual Studies in Photorealistic Augmented Reality. In *Proceedings of IEEE VR Workshop on Perceptual Illusions in Virtual Environments* (pp. 27–32).
- Kress, B. C. & Cummings, W. J. (2017). 11-1: Invited Paper : Towards the Ultimate Mixed Reality Experience: HoloLens Display Architecture Choices. *SID Symposium Digest of Technical Papers*, 48, 127–131.
- Lee, R. & O’Sullivan, C. (2007). A Fast and Compact Solver for the Shallow Water Equations. In *Proceedings of the Fourth Workshop on Virtual Reality Interactions and Physical Simulations* (pp. 51–57).
- Magic Leap. (2018). Magic in the making. [www.magicleap.com](http://www.magicleap.com). Accessed: 2018-12-11.
- Mallat, S. (1999). *A Wavelet Tour of Signal Processing* (3rd Edition). Elsevier.
- Mei, X., Decaudin, P., & Hu, B. G. (2007). Fast Hydraulic Erosion Simulation and Visualization on GPU. In *15th Pacific Conference on Computer Graphics and Applications* (pp. 47–56).
- Nicodemus, F. E. (1965). Directional Reflectance and Emissivity of an Opaque Surface. *Applied Optics*, 4(7), 767–775.
- Nordeus, Erik. (2018). Water Wakes in Unity with C#. <https://www.habrador.com/tutorials/water-wakes/2-water-wakes/>. Accessed: 2018-12-11.

- Samsung. (2018, December 11). Samsung gear VR. <http://www.samsung.com/global/galaxy/gear-vr/>. Accessed: 2018-12-11.
- Smith, K., Battaglia, P., & Vul, E. (2013). Consistent Physics Underlying Ballistic Motion Prediction. In *Proceedings of the 35th Conference of the Cognitive Science Society* (pp. 3426–3431).
- Taneva, B., Giesen, J., Zolliker, P., & Mueller, K. (2009). Choice Based Conjoint Analysis: Discrete Choice Models vs. Direct Regression. In *ECML-PKDD Workshop on Preference Learning*.
- Tessendorf, J. (2004). Water Surfaces in Games. *Game Programming Gems 4*, 265–274.
- Tessendorf, J. (2008). Vertical Derivative Math for iWave. Retrieved from [https://people.cs.clemson.edu/~jtessen/reports/papers\\_files/verticalderivativesforiwave.pdf](https://people.cs.clemson.edu/~jtessen/reports/papers_files/verticalderivativesforiwave.pdf)
- Um, K., Hu, X., & Thuerey, N. (2017). Perceptual Evaluation of Liquid Simulation Methods. *ACM Transaction on Graphics*, 36(4), 143:1–143:12.
- Unity Technologies. (2018). Made With Unity - Unity. <https://unity.com/madewith>. Accessed: 2018-12-11.
- van Assen, J. J. R. & Fleming, R. W. (2016). Influence of Optical Material Properties on the Perception of Liquids. *Journal of Vision*, 16(15), 12.
- VRBox. (2018). VR BOX 2.0 Virtual Reality 3D Glasses. Retrieved from <https://www.amazon.ca/VR-BOX-Virtual-Reality-Glasses/dp/B01LWRTBEE>
- Vuforia. (2018). Vuforia Developer Portal. <https://developer.vuforia.com/>. Accessed: 2018-12-11.

Yuksel, C. (2010). *Real-Time Water Waves With Wave Particles* (Doctoral dissertation, Texas A&M University).